Volume 18 | Number 16 | 21 August 2018 | Pages 2315–2478

Lab on a Chip

Devices and applications at the micro- and nanoscale

rsc.li/loc

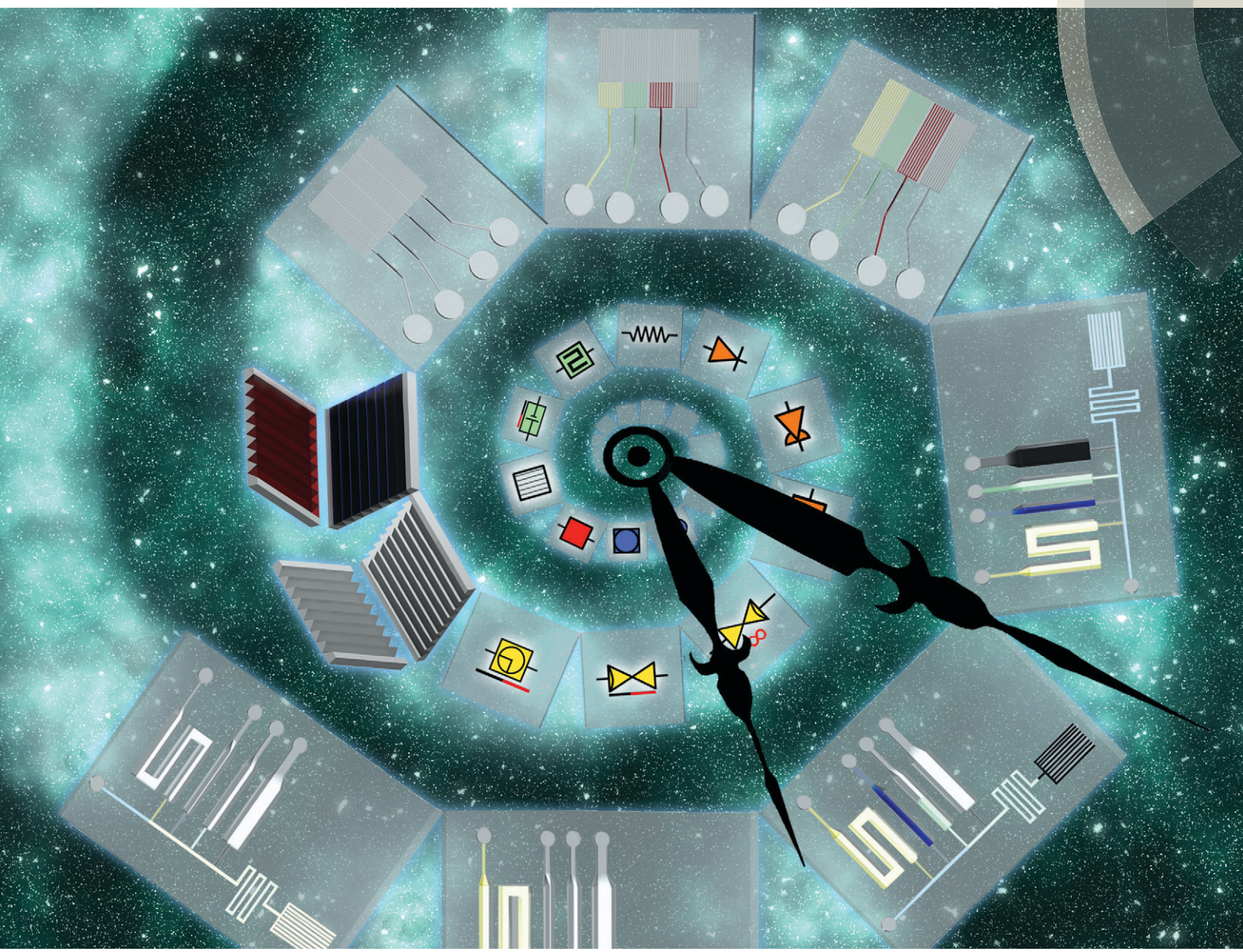

ISSN 1473-0197

ROYAL SOCIETY OF CHEMISTRY

CRITICAL REVIEW

David Juncker *et al.*

Capillary microfluidics in microchannels: from microfluidic networks to capillaric circuits

Lab on a Chip

CRITICAL REVIEW

View Article Online
View Journal | View Issue

Cite this: *Lab Chip*, 2018, **18**, 2323

Capillary microfluidics in microchannels: from microfluidic networks to capillaric circuits†

Ayokunle Olanrewaju, Maïwenn Beaugrand, Mohamed Yafia and David Juncker *

Microfluidics offer economy of reagents, rapid liquid delivery, and potential for automation of many reactions, but often require peripheral equipment for flow control. Capillary microfluidics can deliver liquids in a pre-programmed manner without peripheral equipment by exploiting surface tension effects encoded by the geometry and surface chemistry of a microchannel. Here, we review the history and progress of *microchannel-based* capillary microfluidics spanning over three decades. To both reflect recent experimental and conceptual progress, and distinguish from paper-based capillary microfluidics, we adopt the more recent terminology of capillaric circuits (CCs). We identify three distinct waves of development driven by microfabrication technologies starting with early implementations in industry using machining and lamination, followed by development in the context of micro total analysis systems (μTAS) and lab-on-a-chip devices using cleanroom microfabrication, and finally a third wave that arose with advances in rapid prototyping technologies. We discuss the basic physical laws governing capillary flow, deconstruct CCs into basic circuit elements including capillary pumps, stop valves, trigger valves, retention valves, and so on, and describe their operating principle and limitations. We discuss applications of CCs starting with the most common usage in automating liquid delivery steps for immunoassays, and highlight emerging applications such as DNA analysis. Finally, we highlight recent developments in rapid prototyping of CCs and the benefits offered including speed, low cost, and greater degrees of freedom in CC design. The combination of better analytical models and lower entry barriers (thanks to advances in rapid manufacturing) make CCs both a fertile research area and an increasingly capable technology for user-friendly and high-performance laboratory and diagnostic tests.

Received 2nd May 2018,
Accepted 8th June 2018

DOI: 10.1039/c8lc00458g

rsc.li/loc

1 Introduction

Microfluidic devices are miniaturized liquid handling systems with potential for biomedical applications because of their small sample and reagent volume requirements, potential for efficient mass transport to functionalized surfaces, ease of automation, low-cost, and disposability.[1,2] Although microfluidic chips are small, their operation often requires complex peripheral equipment so that instead of living up to their promise as lab-on-chip devices, the reality resembles 'lab-around-a-chip' limiting the application of microfluidics in point-of-care settings.[3] Capillary microfluidic devices use capillary effects (also called capillary action or capillary force) to manipulate liquids. Capillary effects are governed by the interplay between surface tension of a liquid and the geometry and surface chemistry of its solid support.[4] Capillary microfluidics are often referred to as 'passive' because they typically afford no real-time control over flow, as opposed to 'active' devices with external peripheral control. New descriptors such as self-powered, autonomous, advanced, integrated, and circuit have been associated with capillary microfluidics to reflect their evolving capabilities and inherent advantages related to minimally-instrumented operation and point-of-care testing.

Although the word *capillary* was initially proposed in the context of microfabricated Si microfluidics,[5] over the last decade, the term capillary microfluidics has become strongly associated with the use of porous materials such as paper-based (and to a lesser extent thread-based) devices. Paper-based capillary microfluidics have potential for global health applications and have been widely adopted thanks to low cost and low entry barriers as new devices can rapidly be prototyped using cutters, scissors, or common printers. Porous capillary microfluidics rely primarily on stochastic capillary flow within a network of pores and are well reviewed elsewhere.[6–11] Here, we review microchannel-based, deterministic capillary microfluidics.

Biomedical Engineering Department, McGill University, Genome Quebec and McGill University Innovation Centre, Canada. E-mail: david.juncker@mcgill.ca

† Electronic supplementary information (ESI) available. See DOI: 10.1039/c8lc00458g

There are many different approaches for using capillary effects for flow control in microchannel-based microfluidics. The structurally simplest form of capillary microfluidics use positive pressure generated by droplets deposited at different inlets and outlets to control the speed and direction of flow, with smaller droplets generating higher positive pressures and self-flowing *via* a conduit into larger droplets.[12,13] Positive pressure capillary microfluidic devices are capable of complex operations with minimal user intervention,[14] operate with a small device footprint, and are compatible with robotic pipetting equipment. Nevertheless, the pressures generated are small, and the number of pre-programmed sequential liquid delivery steps without user intervention has so far been limited. In fact, for more complex operations, manual timing of pipetting steps was required.[15] Capillary flow is also applicable to open microconduits and virtual microchannels with liquid confined between horizontal hydrophilic stripes,[16] or suspended between side walls.[17]

Capillary forces are unavoidable at small scales and can significantly affect flow rates even when other active pumping mechanisms are used.[4,18] Capillary phenomena can also be combined with other phenomena, such as electrochemical and electrostatic effects for flow regulation in microchannels.[19–21] In addition, capillary stop valves with hydrophobic features are widely used for flow regulation in centrifugal microfluidics,[22,23] as well as in pressure-driven microfluidics where hydrophobic valves with distinct burst pressures dictate the filling order of different sections of the circuit.[24] More recently, capillary retention burst valves were also integrated within a flexible, wearable, microfluidic device to enable chronological sweat sampling by sequentially guiding liquids into reservoirs, with liquid filling driven by pressure induced by sweat glands and subsequent liquid recovery using centrifugal forces.[25]

The review focuses on self-filling capillary microfluidics that use negative capillary pressure for fluid flow and regulation. Such capillary microfluidics can be designed by combining different elements from a growing library of conceptually idealized 'capillary elements'. The increasingly complex fluidic circuits assembled in a modular manner lead us to propose the term "capillaric circuits" (CCs), which we will use in this review for several reasons. Capillaric can (i) help unequivocally distinguish microchannel-based capillaric microfluidics from paper-based capillary microfluidics, as well as (ii) from capillary electrophoresis (which is a term used to describe electrophoresis in both capillaries and microchannels), and from the (iii) physical capillary as in *glass capillary*, and may help eventually resolve the confusion of search engines. (iv) To convey the idea of a circuit assembled from basic elements,[26] and (v) express the nuance between *capillary* flow as it pertains to the physical phenomena and *capillarics* as it pertains to the circuits and its elements, in analogy to the use of *electric* and *electronic*, and because (vi) it can function as an adjective *capillaric* that is distinguishable from the noun *capillarics*, in much the same way that *microfluidic* is distinguishable from *microfluidics*.

We begin with a brief historical perspective that describes the development of CCs in three waves that are rooted in three distinct fabrication technologies: classical mechanical micro-machining, photolithography and cleanroom fabrication, and more recently rapid prototyping and additive manufacturing. Next, we describe the physical properties governing microchannel-based capillary flow and capillaric elements such as capillary pumps, stop valves, trigger valves, retention valves, and so on, along with their principles of operation. A discussion on how to design pre-programmed, self-regulated CCs follows, organized around sequential delivery of different reagents using various capillaric elements, along with the main applications. We conclude by highlighting recent progress in rapid prototyping of CCs and emerging opportunities in the field.

2 Three waves of development

CCs go back over 40 years with three chronological waves that are linked to three fabrication technologies, including classical mechanical machining, clean-room microfabrication and replication, and rapid prototyping fabrication technologies (Fig. 1).

Microstructures for capillary-driven fluid transport were initially developed not in an academic context, but rather in industrial research labs. These developments primarily appear in patents and are often ignored in the peer-reviewed literature in part because patents were difficult to search for until a few years ago, and also because patents are often tedious to read and sometimes lack experimental details. However, patents from the 1980s document the development of increasingly sophisticated microscale structures for guiding liquid flow *via* capillary phenomena. A number of remarkable designs were patented by Columbus and colleagues from the Eastman Kodak Company. Some of the earliest microchannel-based capillary flow control elements described in patents include: microgrooves for promoting directional capillary-driven transport (Fig. 1A),[27] abrupt geometry changes to stop flow (Fig. 2B),[29–31] self-powered dilution devices that combine capillary effects and gravity for sample dilution (Fig. 2C),[32] matrix plugs for delay and sequential drainage of liquids (Fig. 2D),[33] and advanced capillary pumps with gaps that prevent liquid back flow (Fig. 2E).[34] Some of these patented ideas were rediscovered, implemented using clean-room microfabrication, and published in the peer-reviewed literature sometimes nearly three decades later. For example, Fig. 2A illustrates how microstructures can be used to guide liquid filling fronts to avoid bubble trapping in capillary pumps – an idea originally filed in 1984,[35] which anticipates control of capillary flow in microfabricated devices described below in section 5.6.

Details about the fabrication of early CCs presented in patents was often lacking, or merely hinted at, and was described in the context of lamination (allowing fabrication of thin gaps), or imprinting into polymers, presumably from molds made by micromilling and similar techniques.

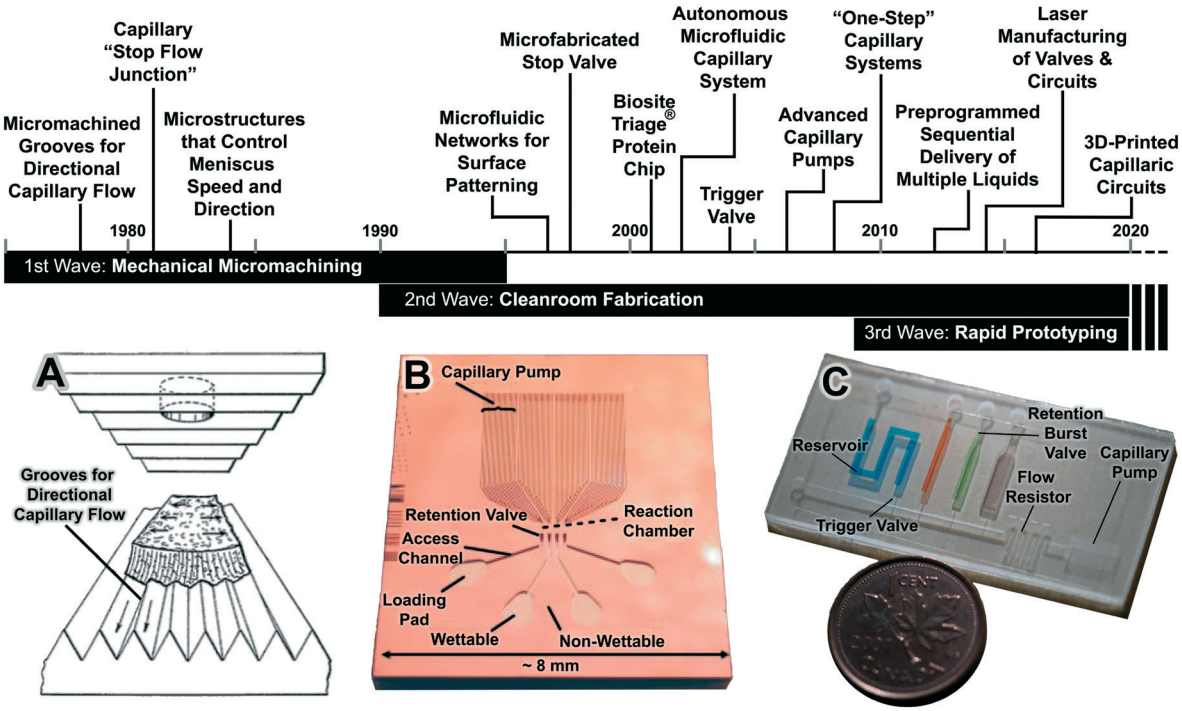

Fig. 1 The three waves of CCs with notable developments highlighted in the timeline. (A) The 1st wave of CCs was developed largely in industrial labs and prevalently relied on mechanical micromachining. (B) The 2nd wave followed the wider use of clean-room technologies, including photolithography, micromachining, and soft lithography for making microfluidics with features down to sub-micrometer resolution, and was developed in the context micro-total analysis systems and lab on a chip. (C) The 3rd wave can be associated with the advances in commercially available and cost effective rapid prototyping systems reaching resolutions of 100–200 μm, adequate for capillary flow, and enabling rapid design and optimization cycles. Adapted with permission from (A) ref. 27, (B) ref. 28 © 2005 WILEY-VCH Verlag GmbH & Co. KGaA, Weinheim. (C) 3D-printed CC from our lab.

Considering that many patents precede advanced silicon microfabrication techniques, it seems safe to assume that they were designed for fabrication using conventional mechanical machining in most cases. Although presented without evidence, many of the ideas in the early patents appear sound. In fact, these early patents may inspire the development of capillaric elements and circuits, notably in the context of additive manufacturing with resolution limitations currently within the same range as that of mechanical machining technologies.

The second wave of CCs rose within the context of micro total analysis systems (μTAS) in the 90s.[36] μTAS was empowered by advances in microfabrication technologies and their widespread adoption for making microfluidic channels with micrometer accuracy in silicon, photoresists, and polymers. Early applications of capillary flow were not for assays, but for micromolding.[37] The potential and power of capillary-phenomena as a powerful alternative to mechanical and electrophoretic pumps in miniaturizing biochemical reactions was presented in a landmark publication by Delamarche and colleagues.[38] They created microfluidic networks that consisted of 1.5 μm-deep microchannels and used capillary forces to fill them, pattern microchannel surfaces with proteins, and deliver immunoassay reagents to patterned surfaces. Design of microfabricated capillaric fluidic elements such as stop valves[39] and capillary pumps inspired by trees and operating *via* evaporation followed shortly after.[40] Microfabricated devices, labelled as *autonomous microfluidic capillary systems*, were developed to implement preprogrammed immunoassays by sequential delivery of liquids from an inlet with newly introduced capillaric fluidic elements known as retention valves.[5] Many subsequent advances were focused on pre-programmed, sequential delivery of samples and reagents for immunoassays using a variety of approaches that will be described in detail in section 6.

Finally, the third (and emerging) wave is rapidly prototyped CCs. Rapid prototyping technologies such as simple craft cutting of tape have long been available, but the lateral resolution of patterned features was often much larger than the thickness of the tapes, thus limiting designs to wide, shallow channels that lacked reliability and only permitted simple fluidic operations.[41] CO_2 laser cutting was recently used as well, with a turnaround time of a few hours,[42,43] but also suffers from low resolution. Advances and popularization of additive manufacturing and stereolithographic 3D-printing have led to multiple commercial systems that claim sub-100 μm resolution with costs a fraction of cleanroom equipment. 3D stereolithographic printing was used to fabricate an array of capillaric elements and circuits with a turnaround time of tens of minutes and at material costs of a few dollars[44] and have already shown the potential for clinically-relevant applications.[45] CCs made by rapid

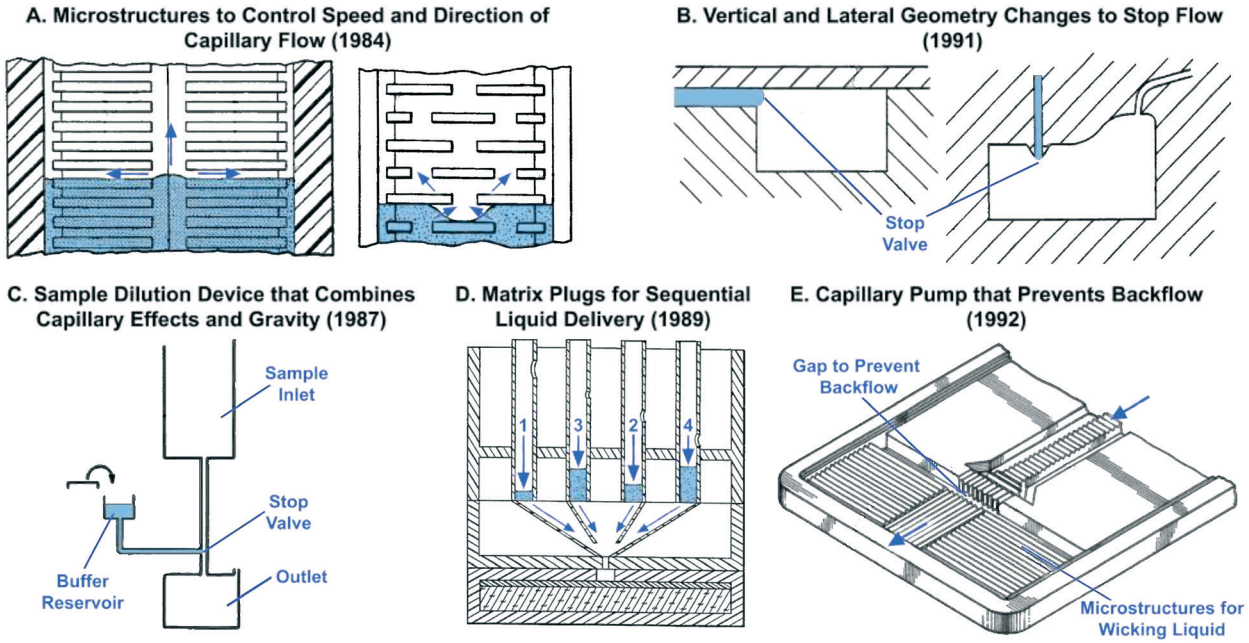

Fig. 2 Examples of early capillary flow devices that were patented decades ago by industrial labs with sometimes striking similarities to results published in recent academic literature. Patent filing dates are listed in parenthesis to reflect the earliest report of each idea. (A) Two examples of microstructures that guide the speed and direction of liquid preventing bubble trapping. (B) Examples of capillary stop valves with abrupt geometric changes to halt flow. (C) Device for dilution and mixing of liquid samples that holds buffer in a reservoir using a capillary stop valve and enables subsequent sample dilution by addition of liquid from an inlet at a higher gravitational potential. (D) Use of porous matrix plugs for pre-programmed sequential drainage of liquids based on properties of porous matrix. (E) Capillary pump structure with microstructures for directional filling and a gap to prevent backflow of liquid towards the inlet. Adapted from: (A) ref. 35, (B) ref. 31, (C) ref. 32, (D) ref. 33, (E) ref. 34.

prototyping are discussed in the eponymous section further below (section 8).

3 Fundamental concepts and parameters

In order to understand the working principle of various capillaric elements and circuits, it is crucial to discuss the fundamental concepts and parameters that underpin their operation.

3.1 Wettability and contact angle

A surface is considered wettable if the contact angle of liquid on that surface is $<90°$. Microchannels with wettable surfaces generate a concave liquid–air interface and a negative capillary pressure that spontaneously wicks liquid into the conduit by capillary action. For angles $>90°$, the interface is convex and the pressure positive pushing liquid out of the channel.

3.2 Capillary pressure

Flow in CCs is driven by capillary pressure or capillary action, and is the reason liquids rise vertically in capillary tubes to a height that depends on their surface tension and the geometry of the tube.[46] Capillary pressure arises at the liquid–air interface in a microchannel as a result of surface tension of the liquid and the curvature imposed by the fixed contact angles which for wettable conduits gives rise to a negative sucking pressure. Most microfabricated channels used in capillary-driven microfluidics have a rectangular geometry due to the use of planar photolithographic and rapid prototyping fabrication technologies. The Young–Laplace equation describes the relation between contact angle, microchannel size, and capillary pressure[47] and can be expressed for a rectangular microchannel as follows:[48]

$$P = -\gamma\left[\frac{\cos\theta_t + \cos\theta_b}{h} + \frac{\cos\theta_l + \cos\theta_r}{w}\right] \quad (1)$$

where P is the capillary pressure, γ is the surface tension of liquid in the microchannel, h, w are the channel height and width respectively, and θ_t, θ_b, θ_l, θ_r are the top, bottom, left, and right contact angles of liquid with the corresponding four microchannel walls.

Eqn (1) and Fig. 3A show that as microchannel dimensions decrease, the capillary pressure increases. The capillary pressure is roughly scaled proportionally to the inverse of the smallest dimension. The capillary pressure can be calculated for each position within a CC, and is realized at the moment the liquid–air interface reaches that position, either during filling or drainage. Thus, by changing the cross-section of different microchannels, one can adjust the capillary pressure and liquid flow within the CC.

There are a few important practical considerations about the contact angles required for proper operation of CCs. It is

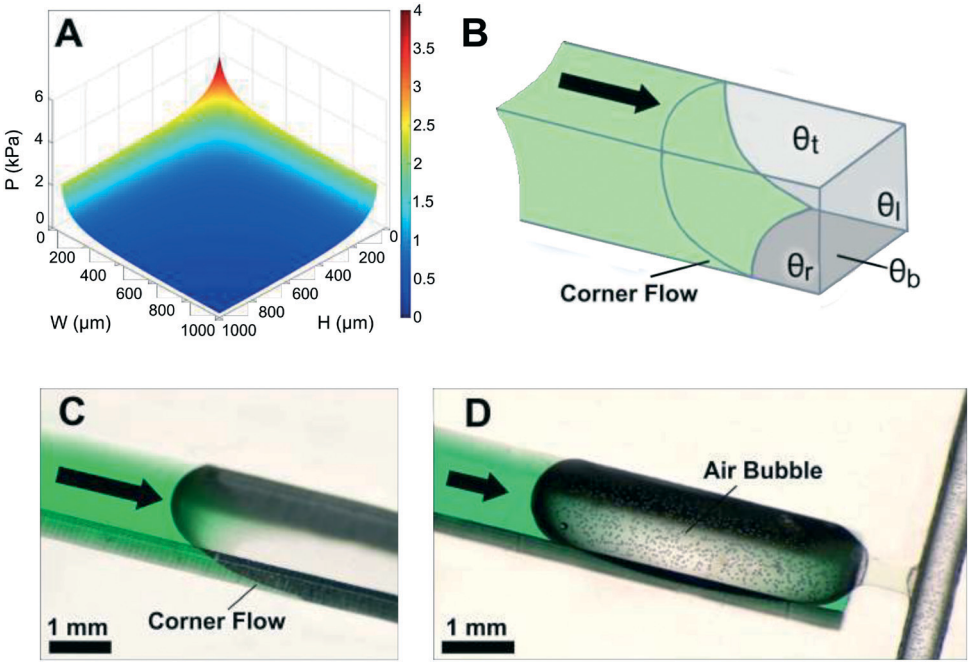

Fig. 3 Capillary pressure and contact angle of liquid in rectangular microchannel. (A) A graph of capillary pressure *versus* microchannel height and width for a rectangular microchannel with a contact angle of water of 40° on all four walls. (B) Schematic illustrating flow in a rectangular microchannel with heterogeneous contact angles θ_t, θ_b, θ_l, θ_r for a hydrophobic top cover and hydrophilic bottom, left, and right walls respectively. Corner flow advancing along the bottom edges of the microchannel is highlighted. (C) Image of green aqueous food dye solution in a rectangular microchannel with hydrophobic top cover (contact angle ≈110°) and hydrophilic bottom, left, and right walls (contact angle ≈30°). (D) Image showing air bubble trapped in microchannel as a result of corner flow proceeding quickly along side and bottom walls and reaching the channel outlet before the bulk of the liquid does – resulting in air bubble trapping, reduction in usable volume, and leading to unwanted large flow resistance in the flow path.

important to have a contact angle significantly smaller than 90 degrees, as the capillary pressure becomes insignificant when approaching 90 degrees, and a single imperfection in the microchannel can lead to local changes in contact angle that could disrupt circuit functionality. Hence contact angles ≤60° are preferred and important to ensure a high yield of functional CCs. Another important consideration is heterogeneous microchannel contact angles when designing CCs with varied geometries. The contact angle on all 4 microchannels walls is equal for CCs built from a single material. However, in many cases one of the microchannel surfaces (typically the sealing layer) is made from a different material that often has a different contact angle (see Fig. 3B). In shallow microchannels with low height-to-width ratios (*i.e.* aspect ratio) flow is driven primarily by the interaction of liquid with the top and bottom microchannel surfaces. For example, when designing a hydrophilic Si microfluidic CC with a hydrophobic polydimethylsiloxane (PDMS) cover, one must avoid very low aspect ratio (height to width ratio) to prevent flow stoppage, especially when there are abrupt geometry changes. The contact angles and geometries of microchannels within the CC must be carefully considered to ensure proper device operation.

3.3 Corner flow

Another important practical consideration when designing CCs is corner flow (or edge wetting) – a phenomenon that arises at the intersection of two wettable surfaces with contact angle <45° – that has the potential to disrupt expected flow patterns. Corner flow is depicted in Fig. 3B and C by the advancing liquid at the intersections of microchannel walls. Corner flow becomes significant at low contact angles (≤30°) and can significantly precede bulk flow in the microchannel depending on channel aspect ratio. Surface imbibition with a liquid precursor film may arise for contact angles approaching 0°.[49] These effects could result in deviations from the pressure predicted in the Young–Laplace equation (eqn (1)).[50,51] For example, corner flow may adversely affect the filling velocity and functionality of capillaric elements. The effects of corner flow are also exacerbated when conduits are fabricated using heterogeneous materials with differing contact angles and geometries with low (or high) aspect ratios. Hence, for CCs with complex geometries and capillaric elements, contact angles in the range of 30 to 60° are recommended to minimize corner flow while allowing for robust filling. Corner flow can also be reduced and almost eliminated by eliminating sharp corners and rounding the edges of the microchannels, but this approach is often difficult to implement owing to limitations in the ability of microfabrication techniques to create microchannels with four rounded corners. Corner flow is an important phenomenon that must be considered to ensure design and fabrication of functional and reliable CCs.

3.4 Flow rate and flow resistance

The flow rate is a crucial parameter to consider when designing CCs because it determines the test time and often also the analytical sensitivity of biochemical assays carried out in CCs. Under the assumption of laminar, steady state flow, and in the absence of gravitational effects, the flow rate Q of liquid in rectangular microchannel can be calculated by solving Navier–Stokes equations and is given as follows:[52]

$$Q = \frac{h^3 w \Delta P}{12\eta L}\left[1 - \sum_{n,\text{odd}}^{\infty} \frac{1}{n^5}\frac{192}{\pi^5}\tanh\left(n\pi\frac{w}{2h}\right)\right] \quad (2)$$

where h is microchannel height, w is microchannel width ($h < w$), ΔP is the difference in capillary pressure across the microchannel, and L is length of liquid in the microchannel.

A further simplified form of the flow rate can be obtained for a flat and very wide channel, where $\frac{h}{w}\tanh\left(n\pi\frac{w}{2h}\right) \rightarrow \frac{h}{w}\tanh(\infty) = \frac{h}{w}$ such that Q can be written as:[52]

$$Q = \frac{h^3 w \Delta P}{12\eta L(t)}\left[1 - 0.630\frac{h}{w}\right] \quad (3)$$

The worst case scenario for the approximation of a flat and very wide channel is the case when $h = w$, at which point the error upper bound is 13%. Meanwhile, the error in this approximation drops very quickly to only 0.2% when $h = w/2$.[52]

The speed at which the liquid meniscus advances in a rectangular microchannel is given by:[53]

$$\frac{\mathrm{d}L(t)}{\mathrm{d}t} = \frac{Q}{wh} = \frac{h^2 \Delta P}{12\eta L}\left[1 - 0.630\frac{h}{w}\right] \quad (4)$$

assuming fully developed Poiseuille flow and using the expression for volumetric flow rate (Q) in eqn (3). The differential equation above can be easily integrated to obtain a relationship between the position of the advancing liquid meniscus, $L(t)$, and the filling time, t, as follows:

$$L(t) = h\sqrt{\frac{\Delta P}{6\eta L}\left[1 - 0.630\frac{h}{w}\right]t} \quad (5)$$

Eqn (5) has the classic square root relationship between filled length and time first described by Washburn a century ago.[54]

Using electrical analogies the flow resistance, R, within a microchannel can be defined as:

$$R = \frac{\Delta P}{Q} = \frac{12\eta L}{h^3 w}\left[1 - 0.630\frac{h}{w}\right]^{-1} \quad (6)$$

Similar expressions can be obtained for different microchannel geometries including circular, rectangular, and infinite slit microchannels.[55] The instantaneous flow resistance and capillary pressure govern the filling of microchannels and are used to derive scaling laws to guide the design of CCs. It is important to emphasize that unlike electronic circuits which are 'pre-loaded' with electrons, the relationship between flow rate and flow resistance changes as liquid fills the circuit. The capillary pressure difference, (ΔP), is the instantaneous pressure at the liquid–air interface which can undergo large variations within a few micrometers if the channel cross-section changes abruptly. Meanwhile the fluidic resistance, R, typically increases monotonically as the microchannel fills, while the overall resistance is dominated by the section with the smallest microchannel height h.

4 Foundations of capillaric circuits

To understand the physical embodiment of capillaric elements and circuits, it is important to first describe the fabrication techniques, materials, and surface treatment methods commonly used in this field. This description not only highlights design constraints but helps to identify potential areas of improvement in CC development, possibly leveraging innovations in adjacent fields like materials science and surface chemistry.

4.1 Fabrication

Currently, the dominant technique for fabrication of CCs is photolithography in cleanrooms. Below we briefly summarize key capabilities and challenges of cleanroom fabrication. One of the most common methods for fabricating capillaric elements and circuits is direct patterning of silicon substrates.[5,56–58] Si CCs are often made by deep reactive ion etching which can create channels and vias with aspect ratios up to 20 : 1 but depends on expensive cleanroom infrastructure and often a slow design-to-device time because of the requirements for photolithography masks and complex fabrication processes.

A simpler and more cost efficient alternative is to use soft lithography. A negative of the CC is made by patterning the channels as ridges in photoresist on a Si wafer, and replicating the pattern into soft and transparent polydimethylsiloxane (PDMS). Upon making a single Si wafer with the positive patterns, multiple PDMS replicates can be made in the lab using common consumables and an oven.[26,59,60] When using Si CCs, PDMS can be used as the sealing (cover) layer because its elastomeric properties allow it to spontaneously and reversibly seal other surfaces. PDMS CCs can be sealed onto glass or any smooth surface, including PDMS itself.[26,44] Although PDMS replication is relatively fast for academic laboratory use (≈4 h), it is too slow and uneconomic for mass production, which can be realized using hot embossing (≈minutes) and injection molding (≈seconds). The slow replication time of PDMS can be circumvented by using a PDMS mold and replicating it into polymers that can be UV-cured

in seconds, such as Norland Optical Adhesive (NOA),[61,62] and off stoichiometric thiolenes (OSTE).[63,64] Even though hundreds of PDMS replicas can be made from a single microfabricated master, there is a high entry barrier because of the need for familiarity with mask design and cleanroom processes to make the master. Whereas some of the cost barriers can be overcome by using lower-resolution photomasks made of flexible transparency films that cost only tens of dollars, the long cycle times between making photomasks and completing the cleanroom-based fabrication remain. Some of the barriers can be further reduced by implementing a low cost photolithography station using (often second-hand) cleanroom equipment suitable for the lower resolution (≥10 μm) features needed, but again at the cost of an initial significant investment.

4.2 Materials and surface chemistry

Many different materials have been used for fabricating CCs including glass, silicon, polymers, and hybrid structures made of multiple materials. Wetting and contact angles of aqueous solutions on materials are fundamentally important in capillary microfluidics. Although glass and silicon dioxide are hydrophilic, with contact angles of 25° and 52° respectively,[65] most polymers commonly used for microfluidic fabrication are only mildly wettable or hydrophobic as is the case with PMMA and PDMS that have contact angles of 71° and 107° respectively.[66] Thus, surface treatment is required to obtain wettable surfaces that provide sufficient capillary pressure for self-powered filling and drainage of capillaric elements and circuits.

One of the most common techniques for rendering CCs hydrophilic is gas phase treatments that expose the substrate surface to plasma, ozone, or UV light. High energy oxygen radicals are generated and bombard the substrate surface oxidizing it and rendering it hydrophilic. Gas phase treatments are quick and in <10 seconds can provide a hydrophilic CC surface. Another commonly used hydrophilization technique for CCs is vacuum-based or solution-based surface grafting of silanes with hydrophilic end groups, including notably polyethylene glycol (PEG) silanes with anti-fouling properties.[5,58] PEG silanes yield contact angles that fall within the 30–60° range that is optimal for implementing many capillary flow functions.

An important challenge to surface treatment of CCs is the stability of the surface coating. Silicon, glass, and many polymers maintain a highly stable and wettable surface after treatment with plasma or silanes; however silicones such as PDMS rapidly revert to a hydrophobic state after plasma oxidation or silane treatment.[67] UV curable polymers such as Norland Optical Adhesive (NOA) are a useful alternative to PDMS for rapid prototyping in laboratory settings while retaining a stable hydrophilic surface.[61,62] The variety and quality of techniques available for rendering CCs hydrophilic is a large topic that would warrant its own review.

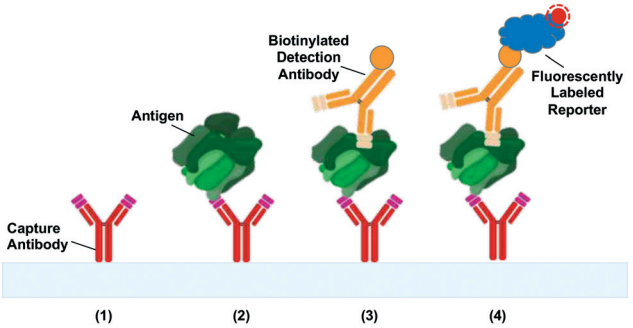

Fig. 4 Schematic of a typical sandwich immunoassay. The following steps are required: (1) patterning of capture antibodies on the surface of the reaction chamber, (2) flow of antigen over the patterned reaction chamber, (3) flow of biotinylated detection antibody, (4) flow of fluorescently-labeled reporter (*e.g.* secondary antibody or streptavidin).

4.3 Brief primer on immunoassays

The most common application of CCs to date is the automation of liquid handling steps for bioassays. Fig. 4 shows a schematic of a sandwich immunoassay – one of the most prevalent immunoassays in clinical and research use.[68] We provide a short summary of the typical liquid handling steps required for sandwich immunoassays in order to help understand the development of capillaric elements and circuits. First, capture antibodies are immobilized on the surface of the reaction chamber. Next, sample is flowed through the reaction chamber. Then biotinylated detection antibodies are flowed through, followed by fluorescently-labelled streptavidin that provides a signal readout. Washing and surface blocking/passivation steps may be included between assay steps to minimize non-specific biological interactions, thereby reducing the background signal. Imaging of the assay result is carried out after the liquid handling steps are complete.

Numerous variants of the basic immunoassay exist.[69] For example, directly fluorescently-labelled detection antibodies can be used to minimize the number of liquid delivery steps. Another possibility is to use detection antibodies conjugated to gold or polymer nanoparticles for visualizing results with the naked eye as is widely used in paper-based microfluidics and lateral flow assays, including pregnancy tests. Alternatively, enzyme linked immunoassays (ELISA) can be performed to provide signal amplification and/or colorimetric readout as has been demonstrated in paper-based microfluidics.[70] Regardless of the variant, the key requirement is sequential delivery and removal of reagents in the reaction chamber to allow assay completion. In a laboratory setting, an operator can intervene to pipette solutions for each assay step, but in a point-of-care setting, it is desirable to minimize the number of pipetting steps, and thus the patient sample is often used to rehydrate pre-dried reagents. CCs have been developed using both wet and pre-dried reagents making them useful either as research tools or point-of-care diagnostics. Application of CCs to immunoassays is discussed in further detail in section 7.

5 Capillaric elements

A stereotypical CC is shown using symbolic representation adapted from electronic schematics (Fig. 5).[26] Conceptually, CCs can be designed by combining individual capillaric elements to form *autonomous* microfluidics for self-powered and self-regulated liquid delivery. Flow is generated by the self-filling property of the microchannels and sustained by capillary pumps after the microchannels are filled. Flow resistors, stop valves, trigger valves, retention valves, and retention burst valves regulate flow. The design of inlets and vents is crucial to ensure entry and exit of liquid in microchannels. Meanwhile the patterned reaction chamber ensures capture of analytes of interest during a bioassay. The functionality of capillaric elements is realized only when the liquid–air interface reaches those elements either during filling or draining of different branches of the CC; once filled, capillaric elements simply act as flow resistors. Hence, as described in eqn (6), the flow resistance gradually increases as liquid fills different sections of a CC, and decreases as liquid drains from different sections. Below, we review the conceptual operating principle of various capillaric elements used to generate and regulate flow in a CC. We discuss the design, capabilities, and limitations of capillaric elements (theory) and components (practical implementation).

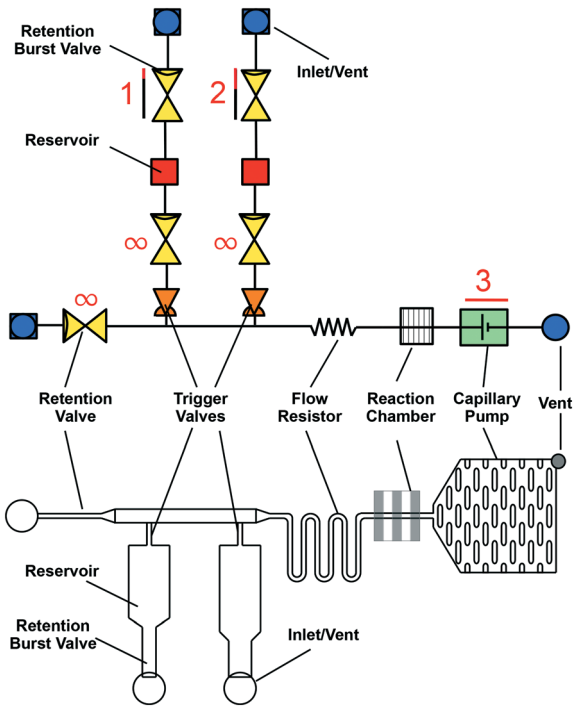

Fig. 5 Symbolic (top) and schematic (bottom) representations of a microfluidic circuit consisting of several capillary fluidic elements including: capillary pump, trigger valve, retention valve, retention burst valve, flow resistor, inlets, and vents. Fig. S1† provides an editable version of this image as well as symbolic representations of individual capillaric elements to enable others to re-use and edit our proposed symbols and highlight their own modular designs.

5.1 Vent

Air vents are a crucial yet sometimes overlooked component of CCs. An air vent is required to ensure that liquid introduced into a CC is able to fill microchannels by displacing air. In fact, some CCs use closed vents to allow liquid preloading and prevent flow in a CC until the user is ready to start the assay.[71] Vents are often realized simply by sealing only part of the CC with a cover leaving the rest open to air, or by drilling access holes through the cover or the CC itself. Vents should be rendered hydrophobic to prevent them from filling with liquid and stopping flow. However, filling of vents with liquid may also be used as a designed feature where flow stops in a pre-programmed manner once the vent is filled. Vents may also be used at intersections within the circuit to prevent air bubble trapping if a second liquid is meant to flow in a pre-filled channel. Vents are a simple yet indispensable part of CCs required to ensure fluid flow.

5.2 Inlet

Inlets are the entry ports for liquids into a CC. They serve as the user interface and the world-to-chip interface. Inlets for laboratory prototype CCs are often patterned onto the substrate surface along with the microchannels, typically as wide and shallow structures that are left open after the microchannels are sealed.[5,58,62] These exposed inlets are easy to fill in a laboratory setting using a pipette. However, point-of-care devices are typically designed so that inlets can be filled easily by untrained users, sometimes by applying sample from a finger prick directly onto the inlet.[72] When necessary, inlets can also be supplemented with a blood-plasma filter to remove blood cells and allow only the liquid sample to enter the CC.[58,72] When designing inlets one must consider the nature of the sample and how the test will be used.

There are a few practical challenges to consider when designing inlets. One of the main failure modes of inlets in CCs is the possibility of cross-flow and cross-contamination between different inlets if the surface of the CC is too hydrophilic. For example, liquids can spread from one inlet to another along the substrate surface or *via* corner flow at the intersection between the device cover and the CC surface. To better guide liquid into the inlets and to prevent cross-flow between separate inlets, the top surface of the CCs near the inlets can be made hydrophobic while keeping the microchannels and inlets hydrophilic (see Fig. 1A).[73] Another practical consideration is that the high capillary pressure at microchannel corners can result in unwanted liquid retention and, upon evaporation, can lead to liquid pumping from microchannel conduits back towards inlets. General strategies for addressing corner flow are described in section 3.3. Inlets can be designed to avoid corner flow by literally removing them, and using virtual inlets without any features and applying liquids directly to a narrow conduit protruding laterally beyond the edge of the cover.[45] Rounded inlets can also be milled as vertical holes in the microchip cover (or from the back of the chip) to provide large and easy to manufacture

rounded features. Inlets are a simple, yet essential part of CCs and attention to detail is required to ensure that their design is user-friendly without interfering with subsequent fluidic operations.

5.3 Reservoir

CCs often include reservoirs, microchannels designed primarily to hold – and in many cases to subsequently release – a precise, predetermined volume of liquid. Reservoirs are usually closed microchannels that guide liquids from the inlet towards other capillaric elements. Depending on the intended application, reservoirs can be very small with volumes in the picoliter range[5] or very large with volumes up to 100 μL.[45] Reservoirs typically have low flow resistance and low capillary pressure so that they are quickly and easily drained. Reservoirs can also be connected to air vents in a CC, so that flow is not triggered in a desired region of the CC until a particular reservoir is emptied as described in section 6.3.[74] Care must be taken to minimize evaporation of liquid from open reservoirs and to prevent potential cross-contamination of sample or unwanted exposure of the sample to the operator when biological samples like whole blood are used.

5.4 Reaction chamber

Reaction chambers are the regions within a CC where biochemical assays take place. Like in active microfluidic systems, mass transport and efficient analyte capture must be considered when designing a reaction chamber. Reaction chambers in early CCs often consisted of straight microchannels with capture reagents patterned on the PDMS cover.[5,38] The self-sealing property of PDMS combined with the negative pressure of CCs ensure reliable sealing even in the presence of adsorbed proteins on the PDMS cover. Other reaction chambers have integrated spiral or zig-zagged micromixing structures to increase the incubation time of sample and reagents.[58,75] Similarly, in one demonstration, spiral microchannels were fabricated into the reaction chambers of 96-well plates to provide increased surface area, efficient mass transport, and compatibility with a standardized immunoassay format while also leveraging the benefits of CCs.[76] More recently, functionalized microbeads have been used to increase surface area and improve the efficiency of mass transport within CCs.[45,77–79] Beads can be readily functionalized in batch mode while reducing issues related to surface anisotropy, depletion, and edge effects that can afflict surface-coated conduits and confound assay results. Conversely, bead barriers must be included in the CC, and the CCs pre-filled with bead solution beforehand, without compromising surface chemistry following drying of the delivery solution[78,79] or then delivered on-the-fly during the assay.[45] Reaction chambers must be designed keeping in mind the analyte concentration that needs to be detected, liquid delivery within the CC, and the user-friendliness of the CC.

5.5 Flow resistor

Flow resistors naturally arise from the viscous flow resistance of liquid flowing through a microchannel, and are an important design consideration for any microfluidic chip (see eqn (6)). Flow resistance can be tuned by adjusting the cross-section and the length of the microchannel to obtain the desired flow rate in different channels under constant pumping pressure.[80] However, changing microchannel dimensions can affect both the capillary pressure and the flow resistance. For example, a rectangular microchannel with the height significantly smaller than the width ($h \ll w$) has a capillary pressure proportional to $1/h$ (see eqn (1)) and a flow resistance proportional to $1/h^3$ (see eqn (6)). Thus, decreasing microchannel height increases capillary pressure but increases flow resistance more significantly leading to an overall reduction in flow rate of $1/h^2$ and in flow speed of $1/h$.

A way to reduce the resistance without decreasing the capillary pressure is to use multiple parallel microchannels, and in doing so the flow resistance could be varied systematically to investigate the effects of longer incubation time on the detected signal after an assay.[81] Serpentine flow resistors are also used as mixers within CCs because they provide long residence time that allows diffusive mixing.[75,81] Systematic differences in flow resistance of parallel microchannels branching from the same flow path were used to create "reagent integrators" for rapid and efficient dissolution of dried reagents while retaining a small footprint for the mixing structure.[82] In addition, flow resistors are used to provide a capillary pressure drop, similar to the voltage drop across an electric resistor to regulate capillary pressures in a CC and regulate sequential bursting of retention burst valves (RBVs) as described in section 6.[26,44]

5.6 Capillary pump

Capillary pumps, Fig. 6, fulfill essential functions in a CC. They draw sufficient sample and reagents to complete a reaction and often also simultaneously serve as waste reservoirs for those liquids. Capillary pumps need to ensure a steady flow rate in CCs. To ensure a steady flow rate, capillary pumps should provide a constant, predetermined capillary pressure regardless of filling level. This implies that the

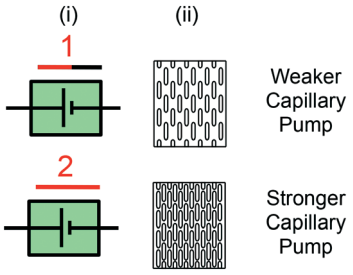

Fig. 6 (i) Symbolic and (ii) schematic representation of capillary pump. The spacing between microstructures in the pump determines its capillary pressure. Stronger capillary pumps have more closely spaced microstructures.

pump should not significantly add to the flow resistance of the overall circuit. Early designs aimed at minimizing the flow resistance of the capillary pump had structures with multiple parallel channels that formed arborescent structures reminiscent of trees (Fig. 7A).[5,83] Many different geometries of microstructures in capillary pumps have since been investigated (Fig. 7B).[84]

Capillary pumps also need to meter a precise volume of liquid in CCs. However, as can be seen in eqn (1), capillary pumps must have small features (sometimes only a few

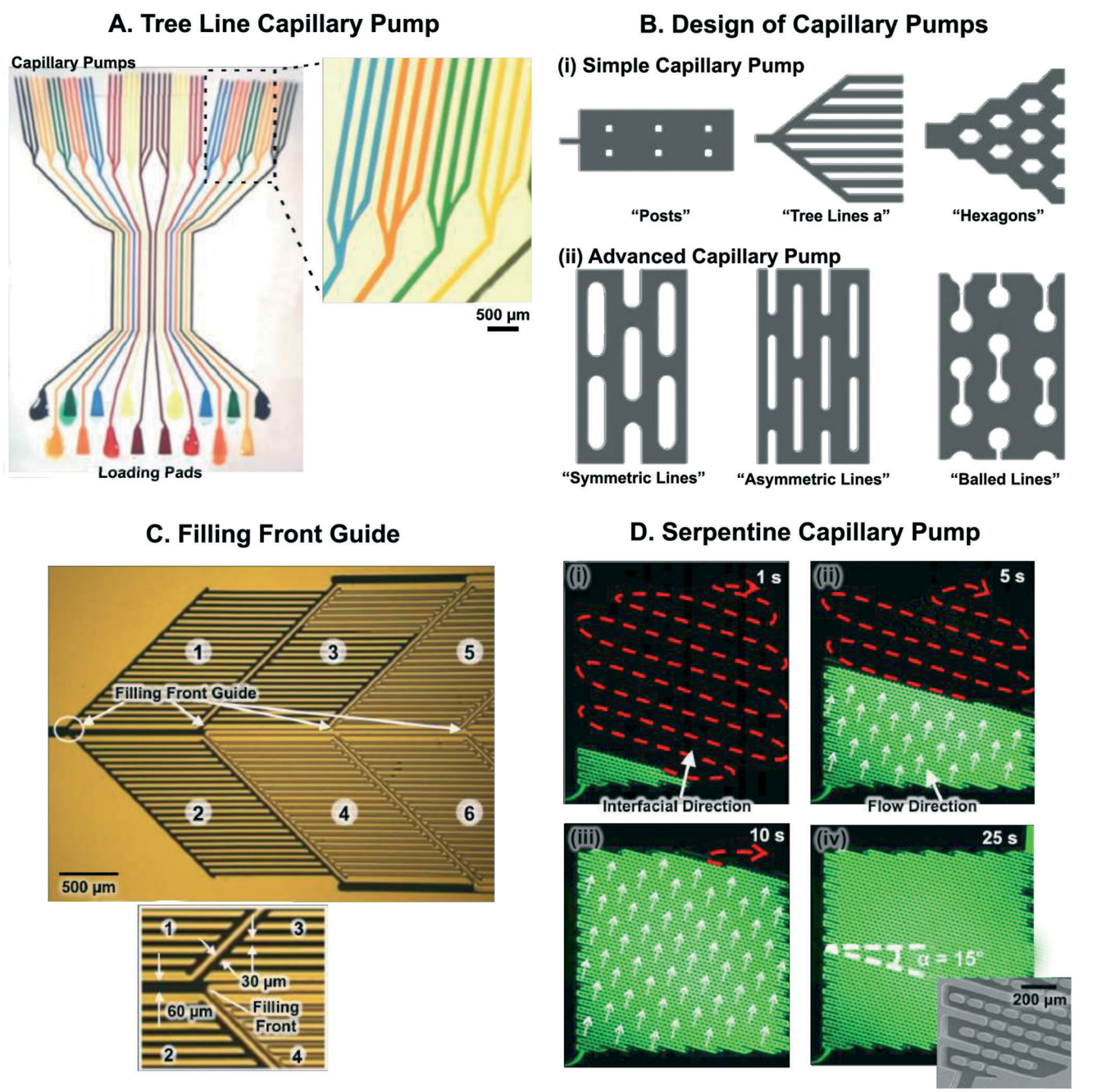

Fig. 7 Microstructure arrangements for capillary pumping and guiding the liquid filling front. (A) 16 CCs – each having a triple tree line capillary pump – reminiscent of branching structures in plants and trees, used for pumping liquid for performing immunoassays. (B) Microstructures for simple and advanced capillary pumping. Microstructure shape and arrangement can be adjusted to guide liquid filling front. (C) Filling front guide designed to distribute liquid into six zones within a capillary pump. Liquid fills higher capillary pressure side channels (30 μm wide) before filling the lower capillary pressure central channel (60 μm wide), thereby ensuring bubble-free and complete pump filling. Zones filled with liquid appear dark. (D) Serpentine capillary pump consisting of micropost arrays with spacing such that there are zones of low and high capillary pressure. This results in movement of the liquid filling front in a serpentine manner without trapping air bubbles. Inset in (iv) shows close-up SEM image of serpentine pump. Adapted with permission from: (A) ref. 83 © 2010 Springer Nature, (B) ref. 84, © 2007 Royal Society of Chemistry, (C) ref. 57 © 2007 Springer-Verlag (D) ref. 85 © Springer-Verlag.

micrometers wide) to generate high enough capillary pressure to drive flow in a CC. Feature sizes on the order of a few tens of micrometers are required, which are etched vertically into Si to a depth of a few hundred micrometers. Aspect ratios up to 10 : 1 and open ratios of 50% or so are possible while ensuring mechanical robustness, yet even a volume as little as 1 μL still results in a capillary pump footprint as large as ≈1 cm^2. At the same time, pumps need to be covered to minimize evaporation, and the resulting large width and comparatively shallow depth capillary pump geometry can result in unwanted trapping of large air bubbles in the centre, and large losses of liquid capacity of the pump (see Fig. 3D). Indeed, as liquid preferentially flows along the edges of the wide area structure it will reach the outlet before filling the centre, thus trapping an air bubble and introducing significant metering errors.[84,85]

Arborescent (tree line) capillary pumps fill effectively while avoiding trapping of bubbles, but the flow resistance of pump lines increases monotonically as the size of the pump increases. In addition, the branching points result in wider gaps that the liquid meniscus must navigate, effectively lowering the capillary pressure at those points. As described in Fig. 7B, advanced capillary pump designs with arrays of microfabricated structures were developed to avoid issues related to branching points. These micropost arrays also have larger open (or void) ratios than lines, enabling them to hold more liquid within the same device footprint.

To increase the capacity of capillary pumps, evaporation was used to continuously pump liquid through a CC, similar to the way that trees combine capillarity and evaporation.[40,86,87] Porous materials (such as paper) were also placed on top of the capillary pump to increase its volume capacity.[44,73,88] Porous pumps provide large volume capacity while retaining small device footprints. If the paper pump completely covers a section of the capillary pump, then the paper pump determines the capillary pressure. But if there is an open conduit section, then it may act as a shunt that gets drained if the capillary pressure is too high in the paper. Paper pumps can also be patterned to provide variable and preprogrammed flow rates.[88,89] It is important to ensure good contact between the paper and the capillary pump for proper flow control as air gaps can create large flow resistances that slow down the flow rate. Using an initial liquid priming step to wet the paper pump before subsequent liquid delivery can help to address this problem.[44,88] Synthetic microfluidic paper with well-controlled arrays of interlocked micropillars was developed in polymer and demonstrated to provide improved performance compared to conventional porous materials.[64] Hydrogels[90] and superabsorbent polymers[91,92] were also used as pumps to drive capillary-driven flow.

5.7 Filling front guides

Filling front guides are used for guiding the path of the liquid front and sometimes the bulk liquid, through a predetermined path within a CC. Liquids fill narrower, higher capillary pressure gaps before filling wider, lower capillary pressure gaps. This fact is exploited by filling front guides to ensure efficient and bubble-free filling of CCs. Interestingly, the first capillary-phenomenon based liquid guides were realized on glass using silane chemistry, forming 'invisible' liquid guides that were filled by positive pressure as well as capillary flow.[16] Another early demonstration used Si chips with hydrophilic conduits sealed on a hydrophobic glass slide, thus supporting spontaneous filling while confining the liquid to the microchannel.[93] By physically moving capillaric components, it is also possible to trigger and guide capillary flow by moving a CC towards a surface to form a narrow gap, and thereby establish a capillary bridge connecting an inlet to a capillary pump and triggering flow on demand by mechanical movement.[94]

More recently, filling front guides have been used to control the filling of capillary pumps. For example, Zimmermann *et al.* designed multi-compartment capillary pumps with a larger 60 μm wide central channel (which they termed a delay valve) connecting compartments that were made up of narrower, 30 μm wide side channels. Filling of a downstream compartment could only be initiated after the previous one was filled entirely (Fig. 7C).[57] An advantage of this structure, is that the bulk flow proceeds centrally through the central, wide channel to downstream compartments, thus minimizing the overall flow resistance of the capillary pump. Deterministic control of the liquid filling front can also be obtained by precisely controlling the position and spacing of microstructures within a capillary pump. By precisely arranging microstructures to create zones of high and low capillary pressure, liquids could be routed either in a serpentine manner (Fig. 7D), or in a leading edge manner where liquid moves along one edge of the pump before filling each row.[85]

Phaseguides are another fluidic component that allow routing of liquids in microchannels.[95,96] Phaseguides are formed using small bumps or dips in microchannels that create a capillary pressure. Phaseguides with different pressure barriers can be used to guide liquid along a desired path. Demonstrations of phaseguides so far were performed with variable positive pressures applied at the liquid inlet; however, they should be compatible with fully self-filling systems powered solely by capillary forces.[97]

5.8 Stop valve

Stop valves halt the flow of liquid in microchannels without external intervention using an abrupt change in microchannel geometry.[39,57] Liquid is stopped at abrupt enlargements in the microchannel cross-section that locally decrease the magnitude of capillary pressure driving flow in the microchannel. The theoretical principles behind the operation of the capillary stop valve have been described in detail elsewhere.[22,39,57,98] Fig. 8A shows the geometric parameters that affect the pressure barrier provided by a 2-dimensional stop valve. The pressure barrier, ΔP, for a 2-dimensional stop valve is given by:[39]

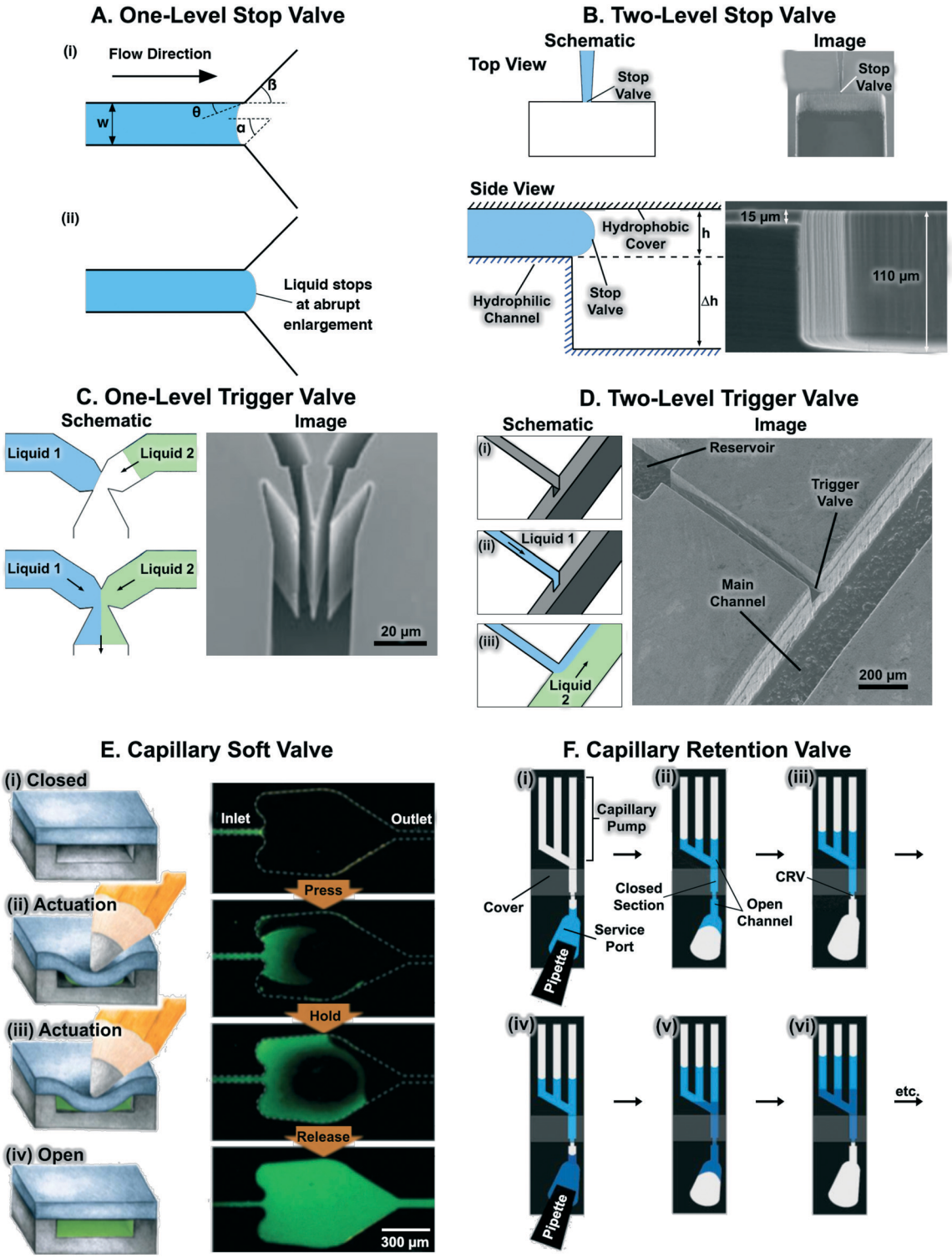

Fig. 8 Schematics and images of capillaric valves capable of stopping flow. (A) One-level stop valve. (i) Schematic of the geometry with key parameters used in analytical pressure calculations (eqn (7)) and schematic of liquid stopped at an abrupt geometry change in a microchannel. (B) Two-level stop valve schematic and SEM image showing abrupt geometry change in both lateral and vertical directions. (C) One-level trigger valve schematic showing how liquid is released when fluid is present at both sides of a trigger valve junction and SEM image of a trigger valve with large height-to-width aspect ratio. (D) Schematic of a two-level trigger valve showing its geometry and operating principle. SEM image showing structure and dimension of a trigger valve. (E) Capillary soft valve also stops liquid at a capillary pressure barrier formed by a wide channel with a hydrophobic PDMS cover. Manual actuation decreases microchannel height, decreasing the pressure barrier, and restarting flow. (F) Capillary retention valve (CRV) allow sequential loading of a capillary microfluidic system. Liquid is pinned at the CRV (step c) because it has a higher capillary pressure than the capillary pump. Adapted with permission from: (B) SEM images from ref. 99 © 2005 Elsevier B.V., (C) schematic from ref. 56 © 2004 Elsevier B.V., SEM image from ref. 57 © 2007 Springer-Verlag, (D) SEM image from ref. 26 © 2013 Royal Society of Chemistry. (E) Ref. 100 © 2012 Royal Society of Chemistry. (F) Ref. 5 © 2002 American Chemical Society.

$$\Delta P = \frac{2\gamma}{h}\left(\frac{\cos\theta - \frac{\alpha\sin\beta}{\sin\alpha}}{\cos\beta + \frac{\sin\beta}{\sin\alpha}\left(\frac{\alpha}{\sin\alpha} - \cos\alpha\right)}\right) \quad (7)$$

where w and h are the width and height of the microchannel leading into the stop valve ($w \gg h$), θ is the contact angle, α is the liquid meniscus curvature in the lateral direction, β is the change in curvature of the liquid meniscus as illustrated in Fig. 8A.

Although stop valves are reliable and simple to incorporate within actively powered hydrophobic systems,[22,39,101] their reliability in capillary-driven systems is often not reported or only described for short durations (*e.g.* 5 min (ref. 43 and 57)). Very low contact angles can result in corner flow that disrupts the functionality of stop valves and depending on the geometry, may lead to bubble trapping (*e.g.* when a wide channel is followed by a constriction, see Fig. 3).

To improve the reliability of stop valves, Glière and Delattre developed two-level stop valves with hydrophilic silicon microchannels and hydrophobic PDMS covers (Fig. 8B). They numerically and empirically characterized the burst pressure of two-level stop valves as a function of microchannel hydraulic diameter and contact angle.[99] More recently, 3-dimensional stop valves were used to pattern antibody solutions within closed microfluidic chips.[102] Nevertheless, stop valves have had limited use in CCs as they typically require external actuation to overcome the flow stoppage.[39] Stop valves can readily be turned into capillary trigger valves (described below) by implementing the flow stop at an intersection with a second (orthogonal) microchannel. This allows flow of the stopped liquid to be resumed simply by adding a liquid to the orthogonal microchannel (Fig. 8C).

5.9 Capillary trigger valve

Capillary trigger valves are modifications of stop valves that enable flow stoppage and subsequent liquid release using capillary flow only. The earliest trigger valve design reported in the literature relied on the merger of multiple microchannels at a junction and required all microchannels to be filled in order for flow to progress, in effect realizing an "AND" logic operation with two or more reagents.[56,57] These early trigger valves were made from silicon and required very high aspect ratios (*e.g.* $\frac{h}{w} = 12.5$)[56] to successfully stop liquid (Fig. 8C). To reduce fabrication constraints and improve reliability, two-level trigger valves with lower aspect ratios inspired by two-level stop valves were developed (Fig. 8C).[26] Instead of having two microchannels narrowing into a junction, two-level trigger valves have microchannels that meet at an orthogonal intersection (Fig. 8D). Two-level trigger valves are more reliable than one level-trigger valves and can robustly stop liquids for over 30 min.[26,44] Two-level trigger valves can also have larger dimensions (up to 1 mm wide) without compromising functionality since the microchannel step height between the two levels can be used to create a sufficient pressure barrier that prevents flow. Further study is required to ascertain the influence of parameters such as liquid surface tension and contact angle on the reliability of two-level trigger valves.

5.10 Capillary soft valve

Capillary soft valves use a capillary pressure barrier formed by a microchannel enlargement to stop flow. Flow is reinitiated by applying manual pressure using a sharp tip on a soft cover that deflects into the channel (Fig. 8E).[100,103] When a user pushes down on the PDMS cover, the channel height is reduced resulting in a local increase in the magnitude of the wicking/negative pressure thereby restarting flow in the microchannel. Although capillary soft valves are relatively easy to fabricate, flow actuation depends on user intervention, which on one hand creates a constraint and limits scalability, but on the other hand allows for interactive flow control, which can be desirable depending on the application.

5.11 Capillary retention valve

Whereas all preceding valves operated at the filling front, and controlled the filling of liquid, retention valves operate at the draining end, and prevent the drainage of liquid from a filled section of the CCs by pinning the liquid *via* capillary pressure. By placing a retention valve at the inlet of a closed microchannel such as a reaction chamber, it is possible to simply load reagents one after the other, as they are drained from the inlet by the capillary pump, while the retention valve prevents complete drainage, entry of air, and drying of the reaction chamber downstream.[5,73,104] Retention valves are realized simply by reducing the microchannel cross-section and generating a capillary pressure that exceeds that of other downstream components such as the capillary pump, ensuring that retention valves cannot be emptied during operation (Fig. 8F). The retention valve constriction has to be of smaller dimension than the capillary pump, thus limiting the range of capillary pressure of the pump and the CC.

5.12 Retention burst valves

Retention burst valves (RBVs), Fig. 9, also operate at the drainage end, but work as programmable pressure fuses, allowing drainage of a reservoir at a predefined burst

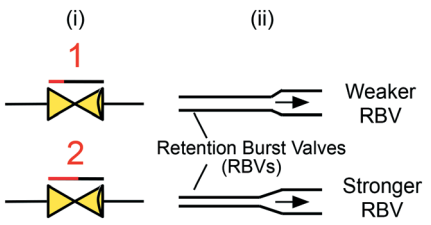

Fig. 9 (i) Symbolic and (ii) schematic representation of retention burst valves. Arrow indicates flow direction.

pressure encoded by the microchannel geometry of the RBV. As illustrated in Fig. 11B, the sequence of reservoir drainage, and hence the sequence of reagents flowing through a downstream reaction chamber, can be pre-programmed by connecting each reservoir to a RBV with a unique burst pressure as discussed below. Similar to retention valves, RBVs are realized by reducing the cross-section of a channel. The precise burst pressure is calculated using the Young–Laplace equation (eqn (1)) and fine tuned experimentally.[26,44] The range of burst pressures that can be encoded is limited by the pressure of the capillary pump – which needs to generate a higher negative pressure than the strongest RBV – and by the largest microchannel dimension that can still generate significant capillary pressure.

Note that for successful sequential bursting of RBVs several conditions must be met: (i) the capillary pressure difference between individual RBVs must be increased monotonically, (ii) the difference in capillary pressure between RBVs must be large enough for only one RBV to burst at a time, and (iii) the overall circuit must be designed such that during flow the pressure at each reservoir remains below the bursting pressure.[44] The second condition can be calculated using an electrical equivalent circuit for the CC. Reliability of RBV performance depends on the precision of fabrication techniques in creating geometric differences between RBVs and may also be affected by surface tension differences between liquids in different RBVs since the surface tension directly influences capillary pressure (see eqn (1)). Also, the reliance of initial RBV designs on high-resolution (≈10 μm) differences in microchannel width required conventional cleanroom fabrication that makes design iteration slow and expensive. We discuss rapid prototyping of RBVs using 3D-printing to vary both the height and width of microchannels in section 8.

5.13 Delay valves

For some applications, it is desirable to delay the flow of one liquid, or to precisely time the delivery of multiple different liquids using delay valves (Fig. 10). One approach to delay flow in microchannels is to use dissolvable thin films as preprogrammed time delays within microchannels. This idea is reminiscent of past work using porous matrices to time the delivery of different solutions (see Fig. 2D). Similar dissolvable delay valving schemes were implemented in paper-based microfluidics using different concentrations of sucrose solution that created time delays for multi-step liquid delivery.[105] The dissolved sugar forms a viscous sugar-rich leading edge that can lead to undesirable effects like flow rate reduction and channel clogging in CCs. This is one of the challenges with implementing dissolvable barriers in CCs, since excess dissolved material at the liquid filling front can build up over time and slow down flow or interfere with immunoassays. To address this concern, Lenk *et al.* incorporated dead-end channels to divert polyvinyl alcohol (PVA) dissolvable barriers at the leading edge of liquid away from the main flow path.[71] Another approach to delaying liquids in microchannels is to incorporate a hydrophobic surface as a barrier within the microchannel. For example, Biosite's Triage™ chip (Biosite was acquired by Alere, which was bought by Abbott) has a "time gate" made of a hydrophobic surface. The delay is used to ensure sufficient sample incubation time[106] and is overcome following the adsorption of proteins at the liquid front that render the barrier hydrophilic.

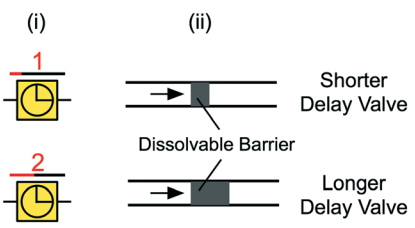

Fig. 10 (i) Symbolic and (ii) schematic representation of delay valves with dissolvable barriers. Arrow indicates flow direction.

6 Capillaric circuits for sequential liquid delivery

After discussing the principle of operation of individual capillaric elements, we now discuss the application of CCs that combine multiple capillaric elements to implement self-powered and self-regulated liquid delivery. The design of CCs aims to provide precise flow control and automate multi-step liquid delivery operations to improve the performance of biochemical assays.

6.1 Sequential delivery with retention valves

The combination of multiple capillaric components – including capillary pumps, retention valves, inlets, and vents – into a single CC (or a capillary system as it was named then) was first proposed in 2002 (Fig. 11A).[5,73,104] The reaction zone of the CC was patterned with capture antibodies using the CC[5] or a simple microfluidic network[38,83] to deposit lines of antibodies onto a PDMS cover layer. Liquids were retained at inlets using retention valves enabling sequential loading of multiple liquids. The circuit by Juncker *et al.* with retention valves was used to perform 16 sequential assay steps (including sample and antibody delivery as well as multiple wash and block steps) for the detection of C-reactive protein (CRP) from 0.2 μL of sample within 25 min.[5] Similar CC designs were used to automate micromosaic immunoassays wherein multiple lines of capture antibodies were patterned onto the reaction zone and exposed to orthogonal flow of analytes, allowing simultaneous detection of multiple analytes with fluorescently labeled detection antibodies within a small device footprint.[73,83,107] For example, using 8 parallel CCs a micromosaic immunoassay was developed to detect CRP and other cardiac biomarkers (including cardiac troponin I and myoglobin) at clinically relevant concentrations from 1 μL of serum within 10 min.[73] Although eliminating the need to remove liquid from the reaction chamber manually, the CC

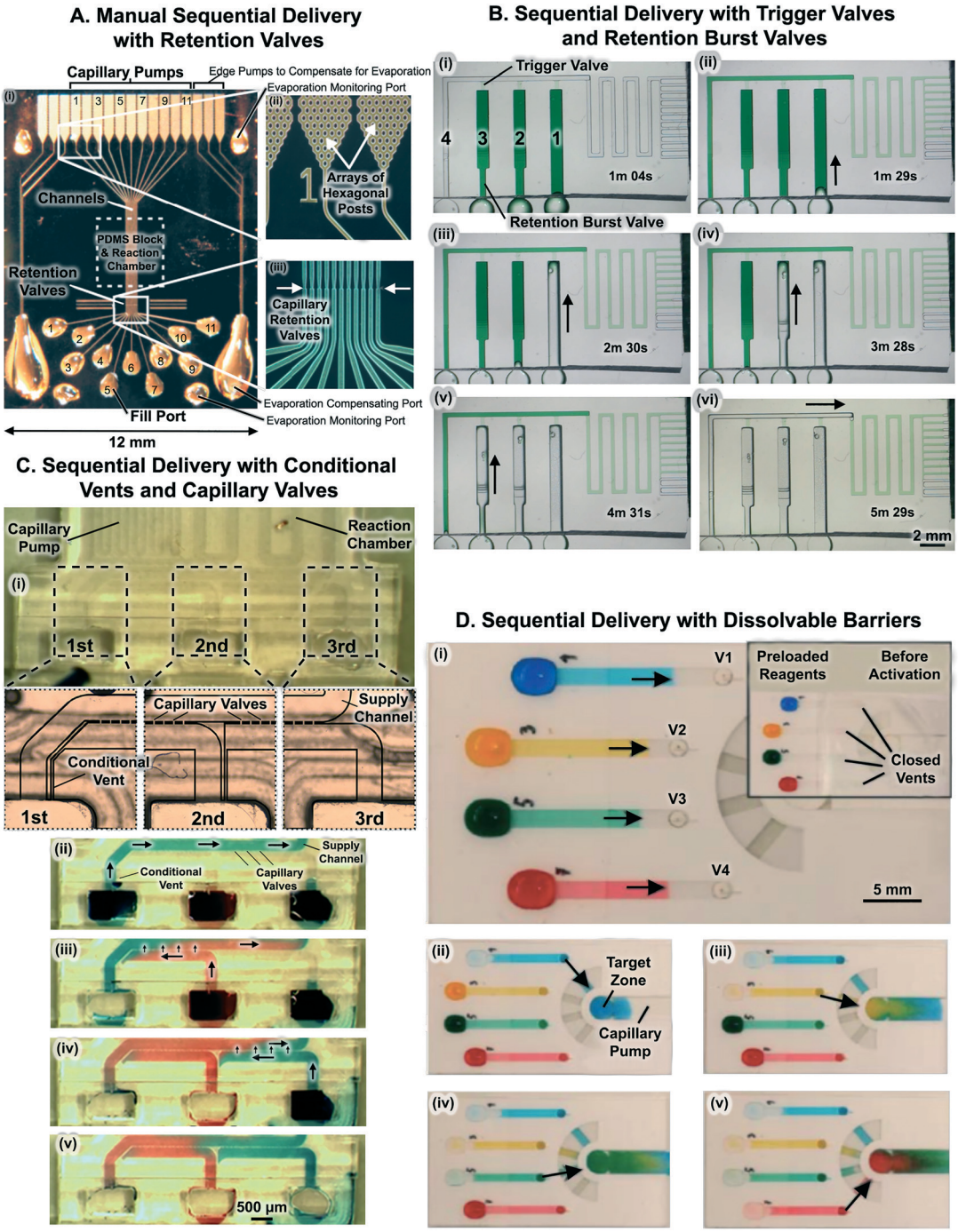

Fig. 11 Capillaric circuits for sequential liquid delivery. (A) 11 parallel CCs for multi-step immunoassays consisting of capillary pumps, retention valves, inlets, patterned reaction chambers on PDMS, and vents. Retention valves prevent drainage of the reaction chamber and bubble trapping when the next solution is applied to the inlet. (B) Timelapse images of sequential liquid delivery in CC with trigger valves and retention burst valves. RBVs drain in increasing order of capillary pressure, with the RBV with the lowest capillary pressure (*i.e.* largest cross-section) draining first. (C) Sequential delivery with capillary valves and conditional vents. (i) Reservoir 1 is connected to reservoir 2 by a microchannel that acts as a conditional vent, and reservoir 2 is connected to reservoir 3 also by a vent. (ii) Upon filling reservoir 1, liquid fills the supply channel and is stopped by capillary valves between the supply channel and inlets 2 and 3. Consequently, the solution flows to the reaction chamber and capillary pumps downstream. When reservoir 2 was filled, liquid did not fill the supply channel, as air outflow through the conditional vent was blocked by residual liquid in reservoir 1. Reservoir 3 was filled similarly, and again liquid stopped at the inlet entrance. (iii) Only upon drainage of reservoir 1, was the vent opened, and solution 2 could fill inlet 2, connect with solution 1 at the capillary valves, and flow through the capillary valves into the supply channel and the downstream units. (iv) Solution 3 then flowed after reservoir 2 was drained. (D) Dissolvable polyvinylalcohol (PVA) barriers for multi-step liquid delivery. The thickness of PVA barriers downstream determines the sequence of drainage of each liquid into the central target zone. Adapted with permission from: (A) ref. 28 © 2005 WILEY-VCH Verlag GmbH & Co. KGaA, Weinheim, (B) ref. 44, © Royal Society of Chemistry. (C) Ref. 74 © 2014 Elsevier B.V., (D) ref. 71 © 2014 Chemical and Biological Microsystems Society.

with retention valves required manual addition of liquids at precise sequences and intervals in accordance with assay requirements.

6.2 Sequential delivery with trigger valves and retention burst valves

Another approach to implementing sequential liquid delivery is to incorporate both trigger valves and RBVs within CCs. Sequential reagent delivery is realized by forming circuit branches that each consist of a reservoir, a RBV, and a trigger valve. The trigger valve connects each circuit branch to a main microchannel leading downstream to the reaction chamber and capillary pump. Fig. 11B shows timelapse images of sequential liquid delivery in a CC with trigger valves and RBVs. Following filling of all reservoirs with reagents in an arbitrary order, sequential drainage is initiated by triggering flow *via* a liquid flowed through the main microchannel which is outfitted with a retention valve at the inlet. As the liquid reaches the capillary pump and is drained from the inlet, flow momentarily stops. As the pressure of the capillary pump propagates through the entire network (as in a hydraulic circuit), the RBV with the lowest capillary pressure bursts leading to rapid drainage of the first reservoir. Importantly, as the reservoir drains, there is a pressure drop in the circuit due to appropriately designed resistances, so that the pressure in the circuit is lower than the burst pressure of the second weakest RBV. Once the first reservoir is drained, a capillary retention valve positioned intermediately upstream of the trigger valve stops the flow, leading to a rise in pressure in the circuit and bursting of the RBV with the second lowest pressure, and so on. Sequential liquid delivery of 8 liquids was demonstrated using CCs replicated from 3D-printed molds.[44] To improve CCs with trigger valves and RBVs, sample aliquoting and storage could be integrated onto the microchip to simplify the initial sample pipetting especially as the number of automated liquid delivery steps increases.

6.3 Sequential delivery with conditional vents and capillary valves

Yet another approach to sequential liquid delivery was realized by Conde and colleagues using a combination of capillary valves (that they termed 'passageways') and conditional vents.[74] Fig. 11C illustrates the CC and shows the capillary valves, an array of 50 μm × 50 μm microchannels connecting various inlets to the central supply channel. Meanwhile, the conditional vents are 40 μm wide × 50 μm deep microchannels that connect reservoirs to one another. The CC is made of hydrophobic PDMS and is covered with a hydrophilic glass substrate. Conduits thus comprise 3 hydrophobic PDMS walls, and a hydrophilic glass cover. Thus unlike most CCs that have either 3 or 4 hydrophilic walls, and 1 hydrophobic cover, here the mostly hydrophobic property of the microchannels results in spontaneous filling of wider conduits while narrower conduits (like the capillary valves and conditional vents) remain unfilled.

As shown in Fig. 11C, the passive valves between channels 1, 2, and 3 act as trigger valves preventing flow of liquid from the supply channel towards reservoir 2 or 3, while allowing flow of liquid towards the capillary pump. On the other hand, the conditional vents connected between reservoirs ensure that a reservoir does not drain until the preceding reservoir has completely emptied. The use of trigger valves and conditional vents is an elegant approach to achieving sequential liquid delivery. However, the same surface chemistry must support filling for wide channels and prevent it for the narrow channels of the conditional air vents, which may affect the robustness and reliability of the CC as small variations in surface chemistry may result in undesirable filling behaviour and device failure.

The same group demonstrated sequential liquid delivery using air bubbles as spacers between orthogonal microchannels connected to a single capillary pump.[108] Liquids were delivered sequentially based on their proximity to the capillary pump and the CC was used to implement an immunoassay. The reliability of the formation of air bubble spacers, and the sensitivity to user manipulation are both of concern given that the presence of air bubbles in microchannels greatly increases their flow resistance.

6.4 Sequential delivery with delay valves

Yet another approach to sequential liquid delivery in CCs is to use dissolvable barriers to control the drainage of parallel microchannels connected to a single capillary pump either by modifying properties (such as the thickness) of the barrier, or by arranging multiple identical barriers in sequence.[71] To enable pre-loading of liquids into parallel channel inlets and simultaneously activate liquid delivery, channel vents were temporarily blocked by sealing them with parafilm. The user pre-loads reservoirs with liquid and when ready to start liquid delivery, removes the parafilm to open up the vents and start the liquid delivery process. As shown in Fig. 11D, sequential drainage of four different liquids from parallel reservoirs was demonstrated. In addition, 19 serial valves were stacked to obtain a delay of up to 11 minutes. Nevertheless, fabrication of individual delay valves can be tedious since different thin film thicknesses need to be manually transferred to specific locations on-chip to achieve sequential drainage.

7 Applications of capillaric circuits

After discussing individual capillaric elements and CCs – composed of multiple capillaric elements – for sequential liquid delivery, we now discuss applications of CCs in biochemical assays. The earliest and most common application of CCs is to automate sandwich immunoassays.[5,58,62,73,75,81,109,110] CCs have several advantages in immunoassay automation, including: (1) small sample and reagent volume (can process nanolitre reagent volumes), (2) precise control over liquid flow speed and direction, (3) self-powered and user-friendly operation, (4) compatibility with transparent substrates enabling sensitive fluorescence or chemiluminescence detection, and

(5) compatibility with micro-patterned reaction chambers to detect multiple analytes within a small device footprint. Below we summarize key applications of CCs and highlight emerging applications.

One-step immunoassays that only require sample addition, and that come with dried reagents spotted along the flow path, were first realized in membrane-based lateral flow assays, and then in microchannel-based microfluidic devices using laminated polymers; both of these technologies were developed in industry and both led to successful commercial products. For example, the Biosite Triage™ chip detects cardiac biomarkers in whole blood (Fig. 12A).[72,106] The Triage™ chip incorporates a blood filter to separate blood cells from plasma. It also has a hydrophobic barrier (or time gate) that is used to control sample incubation time. There are control and assay zones where the immunoassay takes place as well as a waste reservoir for excess liquid. Notably, the laminated microfluidic device provides quantitative readout with high sensitivity and is accompanied by a hand-held reader.

In 2008, a sandwich assay with pre-immobilized reagents in a microfabricated silicon chip was published by the Delamarche group using microscale reagent zones and very small amounts of detection antibodies. CRP was detected in 2 μL of human serum within 10 min.[109] In follow-up work by the same team, 200 μm wide reagent deposition zones, offset from the main flow path, were used to hold dried deposited detection antibodies (see Fig. 12B).[58] Flow mixers were included after the antibody deposition zone to ensure proper mixing of the sample with the reconstituted antibody before reaching the reaction chamber. With this updated design, <1 ng mL^{-1} of CRP was detected in 5 μL of human serum within 14 minutes. The microfabricated Si CC had miniaturized reaction chambers (30 × 100 μm^2) so that multiple reaction chambers could be patterned within a small area.

Over the past five years, there has been growing interest in the development of CCs capable of multi-step liquid delivery operations carried out with minimal user intervention.[26,74,108,111] Multi-step sequential liquid delivery may enable additional wash steps or chemical signal amplification to increase the signal-to-noise ratio of assay results.[26,112,113] Interestingly, sequential flow was also implemented in paper-based microfluidics using two-dimensional networks with varied flow path lengths.[112,114] As described in section 6, there are multiple approaches to achieving multi-step sequential liquid delivery in CCs including the use of capillaric elements such as retention valves,[5] RBVs,[26,44] capillary valves and vents,[74,108] and dissolvable barriers.[71] For example, Safavieh and Juncker developed a CC that enabled not only precise metering of sample volume and incubation time, but also provided different flow rates for sample incubation (slow) and for rinsing (fast) by routing liquids through high and low resistance paths, respectively. To accomplish this, the CC had a flow reversal function that was realized using trigger valves, a second capillary pump, and four RBVs for the sequential drainage of 4 pre-loaded reagents.[26] Using this CC, proof of principle detection of CRP from 1 μL of sample was carried out within 5 min.

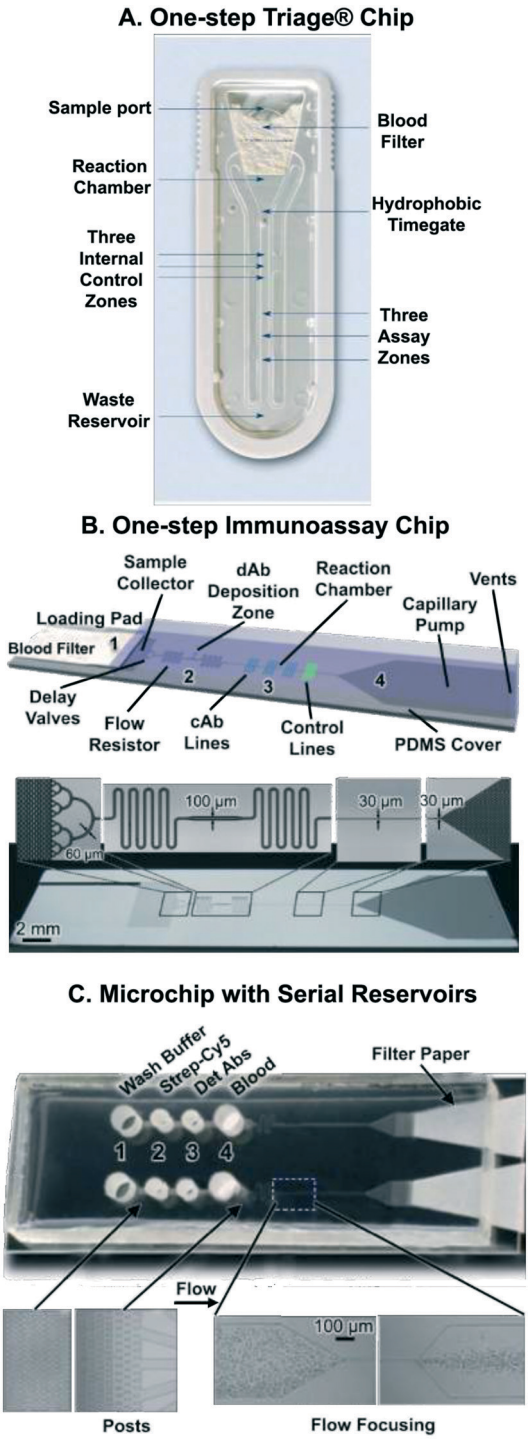

Fig. 12 Capillaric circuits for immunoassays. (A) Image of the Biosite (Biosite was acquired by Alere, which was bought by Abbott) Triage™ chip for one-step immunoassays from whole blood showing its various components. (B) Silicon CC for one-step sandwich immunoassays. Detection antibodies were spotted along the flow path, reconstituted by the sample, and autonomously delivered to the reaction chamber. (C) Microchip for multiplexed protein detection using serially arranged reservoirs pre-loaded with immunoassay reagents and blood. Following reagent and sample loading, the reservoirs drain sequentially from 4 to 1 based on the least resistance principle with limited mixing. Adapted with permission from: (A) ref. 72 © 2002 Wolters Kluwer Health, Inc., (B) ref. 58 © 2009 Royal Society of Chemistry, (C) ref. 62 © 2010 Royal Society of Chemistry.

It is possible to deliver different liquids in sequence without using advanced capillaric elements simply by taking advantage of preference for flow to follow the path of least resistance. A microchip using reservoirs with microposts serially arranged along the flow path results in liquid being drained first from the filled reservoir closest to the pump, followed serially by other reservoirs according to their proximity to the pump (Fig. 12C).[62] Micropost arrays create resistance while also acting as filters to separate blood cells from the whole blood sample. An inertial flow focusing component was included in the microchannel to separate blood cells from plasma (Fig. 12C). Interestingly, the authors used Norland Optical Adhesive (NOA) 63 as the substrate for their CC instead of PDMS, as NOA was found to be hydrophilic after UV curing and unlike PDMS, stably retained its hydrophilicity. Blood sample and immunoassay reagents (biotinylated detection antibodies, fluorescently-labeled streptavidin, and wash buffer) were sequentially delivered through a patterned reaction zone over a 40 minute period using filter paper as a capillary pump. By patterning different DNA-conjugated antibodies onto pre-patterned DNA lines by sequence specific hybridization, a multiplexed assay for detection of 11 proteins in blood was completed. The simple design however faces some trade-offs, such as a need for rapid filling to avoid leaking into adjacent reservoirs, observable mixing between reagents between reservoirs, and a monotonically decreasing (or at best constant) flow rate for different reagents.

Table 1 summarizes a few key examples of CCs demonstrated in the literature. The most common application of CCs to date is immunoassay automation for protein detection, and most frequently cardiac biomarkers. Other targets such as botulinum toxin[75] and whole bacterial cells[45] have also been detected using CCs.

7.1 Hand-held readers for capillaric circuits

For point-of-care diagnostic applications of CCs, it is important that signal readout from CCs is also portable and minimally instrumented. Industrial solutions, for example, the Biosite Triage™ chip has an accompanying reader that provides quantitative results.[72,106] More recently, academic researchers have also developed their own portable readers and integrated them with CCs.[74,115] For example, Novo *et al.* integrated a CC with a microfabricated photodiode array and electronic instrumentation for chemiluminescence ELISA detection of antibody–antigen interactions within 15 min.[74] PDMS microfluidic devices and amorphous silicon photodiode chips were combined within an integrated hand-held unit that also housed a microcontroller and electronic readout circuitry. Another example of hand-held detection was demonstrated by Mohammed and Desmulliez who embedded on-chip planar lenses within PMMA devices and used a custom-made hand-held reader integrating LED illumination and filters for fluorescence detection.[115] The performance of the hand-held optical readers was consistent with fluorescence microscope detection and sensitive enough to provide clinically relevant results.[74,115] For example, the embedded optics developed by Mohammed and Desmulliez achieved a limit of detection of 24 pg mL^{-1} of cardiac troponin I. These examples showcase the potential for combining CCs with hand-held readers and that it may be possible to meet the sensitivity requirement of clinical tests.

7.2 Capillaric circuits for DNA analysis

Beyond immunoassays, CCs have also been used for DNA analysis. CCs consisting of loading pads, reagent deposition zones, capillary soft valves, patterned reaction chambers, and capillary pumps were used for DNA hybridization assays.[100] Biotinylated capture probes and fluorescent intercalating dye were spotted

Table 1 Applications of capillaric circuits. The most popular application of CCs remains protein detection using a sandwich immunoassay, and the examples shown here are representative of typical assay time, sample volume, and limit of detection (LOD). DNA analysis is an emerging application of CCs

Application	Target(s)	Assay time (min)	Sample volume (μL)	LOD	Comments	Ref.
Sandwich immunoassay	C-reactive protein (CRP)	25	0.2	≈1 μg mL^{-1}	Retention valve enabled 16 sequential filling steps	5
	CRP	14	5	1 ng mL^{-1}	One-step assay with dried detection antibodies, re-constituted, and delivered to downstream reaction chamber	58
	11 protein panel (CRP, IL-8, MMP-3, serpin *etc.*)	40	10	20 pg mL^{-1} for IL-8	Antibody–DNA barcode arrays to capture proteins from serum	62
	Troponin I	9	15	24 pg mL^{-1}	Sequential delivery of sample and assay reagents. Integrated on-chip planar lenses for portable fluorescence readout	115
	Whole *E. coli* O157:H7 cells	7	100	1.2×10^2 CFU mL^{-1}	Large-volume CC for immunoassay with packed microbeads for rapid and sensitive bacteria capture	45
DNA hybridization	997-bp PCR product (double-stranded DNA)	10	0.7	20 nM	Uses capillary soft valves to implement DNA hybridization assay	100
DNA amplification (real-time PCR)	BNI-1 fragment of SARS cDNA (and 12 other human gene targets)	30	0.8	10 pg mL^{-1} of SARS cDNA	Surfactant-assisted flow of PCR reagents. Temperature cycling through 94 °C, 55 °C, and 72 °C	116

into reagent deposition zones along the flow path prior to the start of the assay. Double stranded DNA amplified by off-chip polymerase chain reaction (PCR) was added and reconstituted dried reagents and flow was stopped by the capillary soft valve. Next, the DNA was melted at 95 °C followed by cooling, hybridization and manual actuation of the soft valve. DNA target–probe–dye complexes were captured over 100 μm streptavidin receptor lines patterned in the reaction chamber, and could be imaged following rinsing using a fluorescent readout. To prevent air bubble formation during heating, the CC was placed in a chamber at ≈1.5 times ambient pressure.

CCs were also used to perform on-chip DNA amplification by PCR.[116–119] PCR typically requires incubation of samples at three separate temperatures, ≈95 °C for DNA denaturation, ≈55 °C for primer annealing to denote which DNA segments to amplify, and ≈72 °C for enzymatic DNA extension. These heating steps were carried out either with Peltier heaters placed underneath the microchip[116,117] or with thin film heaters integrated directly into the CC.[119] CCs used for DNA amplification have so far been fabricated in hydrophobic materials like PDMS and cyclic olefin copolymer (COC). As an alternative to surface treatment to make the microchip hydrophilic, surfactant was added to the reagents to lower the surface tension, the contact angle, and resulting in capillary-driven flow of PCR reagents in the CC.[116,118,119] Numerical models were also developed to characterize the effect of surfactant addition and the effect of heating on capillary driven flow of the PCR mixture[120] in the CC.[117] These numerical models guided the implementation of PCR in CCs.

CCs for DNA amplification were applied to a variety of targets including the detection of 12 DNA sequences indicative of liver cancer.[116] The results of DNA amplification were monitored in real time based on the increase in fluorescence from intercalating dyes that bind to double stranded DNA. Meanwhile, the DNA amplicon can be identified after PCR by performing a melting curve analysis.[119] PCR with real time monitoring of DNA amplification, using a fluorescent intercalating dye, was completed in 8.5 min. Most of the demonstrations of PCR in CCs so far use relatively simple channel designs, and do not yet leverage advanced liquid handling capabilities available with capillaric elements. One can envision CCs that carry out PCR reactions followed by sequential liquid delivery to complete immunoassays that provide simple fluorescence or colorimetric readout. The challenges that need to be addressed are bubble formation, change in contact angle, and condensation due to heating and the cycles of heating and cooling, and that may lead to CC malfunction. The small dead volume of CCs and the capability to fabricate them with PCR-compatible plastics makes CCs an appealing platform for point-of-care nucleic acid testing. We anticipate more developments in this area in future.

8 Rapid prototyping of capillaric circuits

The third and emerging wave in CC design and development is growing on the back of rapid prototyping. For the last 20 years, fabrication of CCs was predominantly carried out by photolithography in cleanroom environments.[5,26,57,81,108,111] The characteristic dimension of CCs was closely aligned with microfabrication technologies with feature sizes in the range of ≈1–200 μm to generate significant capillary pressure, but limiting the overall volumetric capacity. Motivated by the limitations in resolution of rapid prototyping tools, we and others explored the feasibility of developing larger scale capillaric components, up to 2 mm × 4 mm in cross section, and found that scaled-up capillaric components could be made to work robustly, thus also paving the way for larger volume operations. Below we describe progress towards rapid prototyping of CCs and the state of the art in the field.

8.1 Xurography (razor writing)

Xurography is an inexpensive fabrication technique using a plotter outfitted with a knife or a scalpel to cut patterns in thin polymer films such as tape or transparencies, and is widely used in the graphic arts industry. Xurography has been used for rapid and inexpensive fabrication of microfluidic devices. Xurography was used for fabrication of molds by stacking layers of commercial tape to obtain channel heights ranging from 100 to 400 μm, followed by PDMS replication of microchannels that could be filled by capillary action.[41] Xurography was also used to cut hydrophilic polymer films and spacers that were laminated together with dissolvable polymer films to form CCs for sequential liquid delivery.[71] Although manufacturers of cutting plotters claim resolutions down to 10 μm, in practice the microchannel width that can be reliably fabricated is typically >200 μm.[121,122] While Xurography is inexpensive and accessible, it involves substantial manual operations and alignment to obtain 3-dimensional structures thus limiting its use for fabricating multi-level capillaric components and CCs.

8.2 Laser cutting

CO_2 laser cutting was recently used to directly fabricate CCs into PMMA consisting of capillary pumps with micropillar arrays, timing channels, trigger valves, and integrated microlenses in less than 30 min (Fig. 13A).[42] Laser cutting allows fabrication of multi-level structures, enabling the generation of more advanced capillaric components like two-level trigger valves and retention burst valves.[43,123] Mohammed & Desmulliez experimentally investigated the reliability of two-level trigger valves manufactured by CO_2 laser cutting as a function of geometry and obtained functional trigger valves with widths up to 670 μm.[43] However, the feature sizes obtained with CO_2 laser cutting were limited to >200 μm width. At 200 μm resolution, the cross-section of the microchannels had a triangular Gaussian profile as a result of the shape of the laser beam (Fig. 13B). Rectangular microchannel cross-sections were obtained for widths >400 μm by repeatedly scanning adjacent laser lines over the PMMA substrate (Fig. 13B).[42]

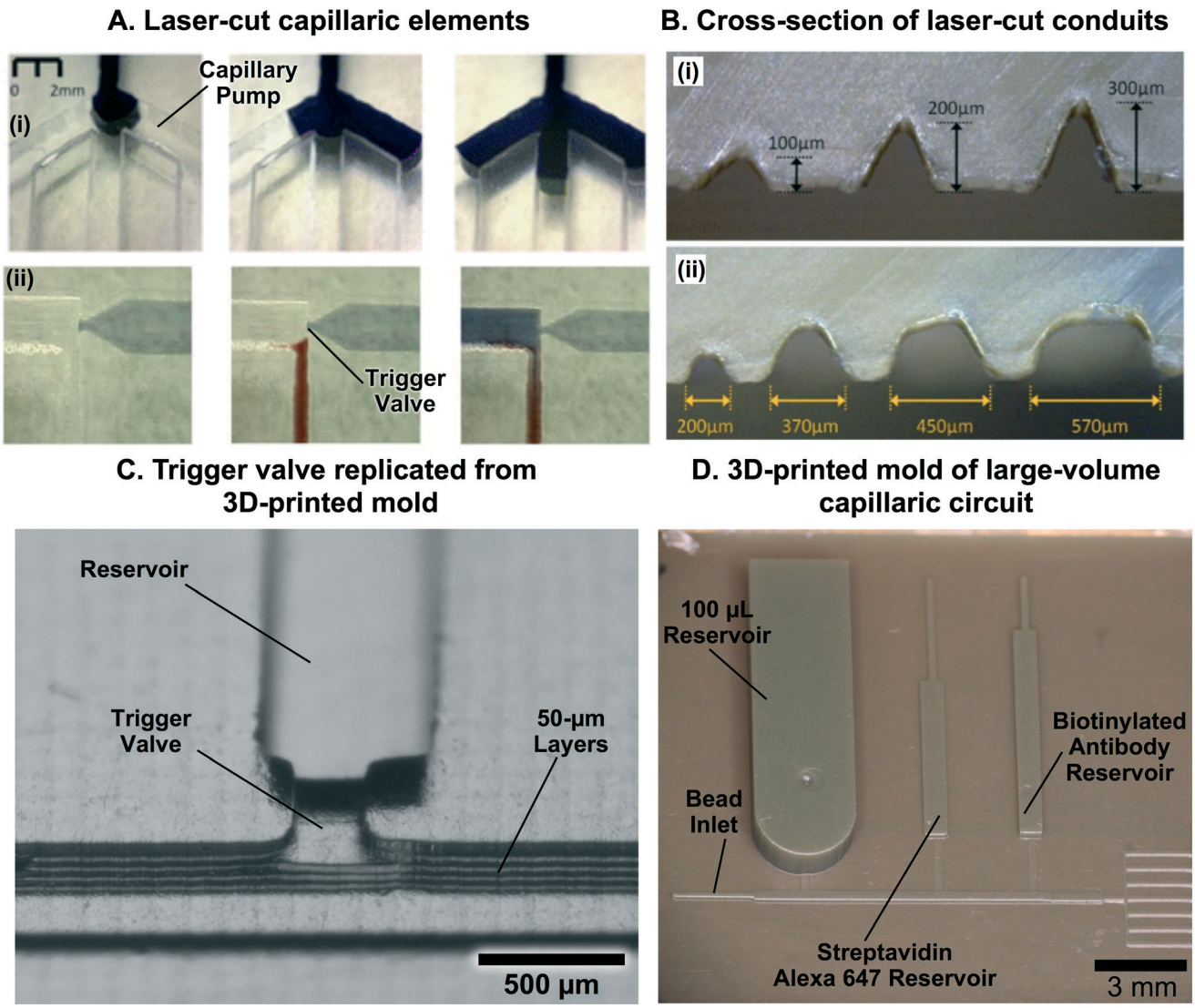

Fig. 13 Rapid prototyping of capillaric components and circuits using CO_2 laser cutting and 3D-printing. (A) Capillaric components fabricated by CO_2 laser cutting. (i) Capillary pump, (ii) trigger valves. (B) Cross-sections of microchannels fabricated by laser cutting. Smaller microchannels (i) have a triangular Gaussian profile that reflects the shape of the laser beam, while (ii) wider microchannels have a more rectangular shape due to repeated scanning of the laser. (C) Front view of 3D-printed trigger valve showing inherent layer-by-layer structure. (D) 3D-printed mold of CC for bacteria detection showing physical realization of structures. Adapted with permission from: (A) ref. 42 © 2013 Springer-Verlag, (B) ref. 42 © 2013 Springer-Verlag Berlin Heidelberg, (C) ref. 44 © 2016 Royal Society of Chemistry, (D) ref. 45 © 2017 American Chemical Society.

More recently, Yan *et al.* directly laser cut a PDMS substrate to fabricate CCs with trigger valves, retention valves, and retention burst valves for sequential delivery of 5 liquids in less than 10 min.[124] Using the CC, they showed colorimetric detection of spiked BSA in synthetic urine with integrated optical readout using a smartphone in 25 min. Although successful, several challenges and limitations are apparent. Laser cutting produced micron-scale surface roughness that compromised the transparency of the PDMS microchannels and also adversely affected the flow profile within the microchannels. Trenches formed at the bottom of the laser-etched microchannels and liquid was observed to be trapped in some of these dead end trenches during rinsing. These results nonetheless showcase the potential of laser writing for rapid prototyping of CCs and improvements might be possible by using higher resolution Nd:YAG lasers[125] or nanosecond and femtosecond lasers,[126] although more advanced lasers have not been used for making CCs to the best of our knowledge.

8.3 3D-printing

Over the past five years, there has been rapid development and adoption of 3D-printing for making microfluidic devices. The low cost and ease of making multi-layer 3-dimensional structures drove this trend. There are different 3D-printing technologies including: fused deposition modelling which involves extrusion from a heated filament, inkjet deposition

and photocuring of materials, and stereolithography-based photocuring of photosensitive resins in a bath. These methods have been well reviewed elsewhere.[127–129] Of these techniques, stereolithography-based 3D-printing has been found to provide the best performance, in terms of resolution (minimum feature size) and surface roughness, when fabricating microfluidic structures.[130] Also, in stereolithographic 3D-printing, there is a trade-off between resolution and throughput. The smaller the feature size that can be obtained, the smaller the overall build area that can be patterned.[127,128] Although several manufacturers now claim to have stereolithography-based 3D-printers with projectors that have resolutions down to 30 μm, the minimum feature size of microfluidic devices obtained is typically >100 μm.[127–130] This is because other factors such as 3D-printer resin properties also significantly affect the feature sizes that can be obtained, and 3D-printers and their resins are rarely customized specifically for microfluidic applications.[131] Recently, the Nordin group developed a custom 3D-printer and resin for microfluidic devices capable of fabricating enclosed microchannels with 18 × 20 μm^2 cross-section, which are sizes that were previously only achievable with cleanroom-fabrication processes.[132]

Despite the growing interest and progress in 3D-printed microfluidics, there have not been many demonstrations of 3D-printing for self-powered and self-regulated CCs to date. There were initial concerns about whether the resolution and structure of 3D-printed channels would be sufficient to make functional capillaric components and support capillary flow. These concerns were addressed with demonstrations showing reliable capillaric components with scaled-up features and optimized geometries. For example, 3D-printed molds for capillaric components and circuits were manufactured in <30 min.[44] The 3D-printed molds were replicated into PDMS, allowing hundreds of devices to be made from a single mold. The 3D-printed microchannels feature a stratified layer-by-layer structure stemming from the step-wise nature of the 3D-printing process (Fig. 13C). Corner flow along these edges is of concern, as described in section 3.3, but is not a major concern when using contact angles between 30–60° that is necessary to establish capillaric fluidic functionality. Indeed, following design optimization, functional and robust trigger valves and retention burst valves were made in PDMS replicates of 3D-printed molds.[44] The digital multi-layer fabrication available with 3D-printing allows the fabrication of RBVs with variations in both the microchannel height and width, accommodating a greater range of capillary pressures and bursting levels, and enabling sequential delivery of up to 8 liquids *versus* 6 for clean-room microfabricated CCs.[44] Furthermore, 3D-printing enabled fabrication of millimeter-scale (13 × 4 × 2 mm^3) conduits with large volume capacity (≈100 μL) within CCs with integrated trigger valves and RBVs for flowing large sample volumes (Fig. 13D). A CC for rapid and sensitive detection of *E. coli* in synthetic urine using microbeads assembled on-the-fly, to provide large surface area that ensures contact of bacteria with functionalized surfaces within the CC, was made as an illustration of the potential and advantage of large volume CCs.[45] The CC for bacteria detection provided results in <7 min, making it one of the fastest bacteria detection tests to date, while meeting the sensitivity requirements for clinical diagnosis of bacteria in urine.

We anticipate many more demonstrations of 3D-printed CCs, given the speed and low-cost of fabrication, and how these enable rapid iteration and development of new capillaric elements and circuits. As the resolution of 3D-printers improves, researchers will need to make fewer design trade-offs and introduce new, complex 3-dimensional features that were not feasible previously.

9 Conclusions and outlook

Over the past three decades, increasingly advanced capillaric elements and circuits were developed and applied to clinically-relevant biochemical applications. This review critically analyzes the history, fundamental operating principles, limitations, applications, and emerging ideas related to capillaric elements and CCs. CCs add to the growing toolbox of miniaturized and user-friendly microfluidics for diagnostic testing that meet global health requirements such as minimal user intervention, sample-to-answer capability, and low cost manufacturing. CCs share many attributes of paper-based microfluidics,[70] but may be pre-programmed to perform some more advanced functions such as the ones typically associated to syringe pumping of reagent droplets,[113] and centrifugal microfluidics.[133] Yet, several challenges must be overcome to enable the use of CCs as portable diagnostics in point-of-care settings. Most CCs currently employ fluorescence detection using conventional microscopes, while long-term reagent storage (*e.g.* pouches) and metering to reduce reliance on precise pipetting have not been implemented yet. Integrated optics[115] and handheld readers,[74] or the integration of simple colorimetric readout will help make CCs more user-friendly and practical.

CCs have been most commonly applied to automate immunoassays for protein detection. New applications such as DNA analysis and detection of whole bacterial cells from large sample volumes have recently emerged, and as more sophisticated CCs are developed one may expect new applications to emerge. CCs could be applied wherever there is a need for hands-off liquid handling with small to high throughput, including: diagnostics, education, cell culture, chemical synthesis, or drug screening. New developments in CCs may enable applications beyond the ones reviewed here, such as capillary-based cooling systems,[134] self-assembly,[135] manufacture of electric circuits,[136] and electronic packaging.[137]

3D-printed CCs rival the fabrication speed and low-cost of paper-based microfluidics while providing deterministic control over microchannel geometry and flow paths. In addition, the digital and standardized ".STL" file format of 3D-printing allows easy sharing of capillaric element and circuit

designs in online databases. A web-based software for automated conversion of symbolic representations of microfluidic circuits into 3-dimensional microfluidic geometries for 3D-printing has already been developed.[138] Such design tools could be adapted to CCs enabling modular design and increased accessibility, allowing us to envision a future where CCs are designed and fabricated as readily as electrical circuits with standardized elements that can be combined to meet application-dependent needs. Ideas that are rapidly prototyped with 3D-printing could then be mass produced by manufacturing high-precision molds with cleanroom microfabrication or micromilling, depending on the specific needs. The latest developments in analytical understanding and lower entry barriers into the field (thanks to rapid prototyping) put us at the start of a rising 3rd wave of development that make CCs both a fertile research area and an increasingly capable technology for making user-friendly and high-performance laboratory and diagnostic tests, as well as opening up the way for new applications. Depending on the intended application, 3D-printing could be used either to print final devices in transparent resins in $<$10 min for on-demand CCs,[139] or for printing molds that can be used for injection molding and thus provide a rapid transition to mass production and potentially very low cost CCs.

Author contributions

A. O. and D. J. conceptualized the manuscript. A. O. wrote the original draft. D. J. supervised, reviewed, and edited the work. A. O. and M. B. prepared and edited figures. M. Y. contributed to Fig. 3 & Table 1. All authors helped to proofread and edit the manuscript. A. O. and D. J. prepared the final version of the manuscript.

Conflicts of interest

There are no conflicts of interest to declare.

Acknowledgements

We thank NSERC and CIHR for funding. A. O. acknowledges the MITACS Elevate Industrial postdoctoral fellowship. D. J. acknowledges a Canada Research Chair. M. B. acknowledges postdoctoral funding from the Fonds de recherche du Québec - Santé (FRQS). We thank Sebastien Bergeron for providing original graphics adapted in Fig. 4. We thank Arya Tavakoli, Oriol Ymbern, and Philippe Lenzen for helpful comments on the manuscript.

References

1 G. M. Whitesides, *Nature*, 2006, **442**, 368–373.
2 D. J. Beebe, G. A. Mensing and G. M. Walker, *Annu. Rev. Biomed. Eng.*, 2002, **4**, 261–286.
3 B. Weigl, G. Domingo, P. LaBarre and J. Gerlach, *Lab Chip*, 2008, **8**, 1999–2014.
4 J. C. T. Eijkel and A. Van den Berg, *Lab Chip*, 2006, **6**, 1405–1408.
5 D. Juncker, H. Schmid, U. Drechsler, H. Wolf, M. Wolf, B. Michel, N. de Rooij and E. Delamarche, *Anal. Chem.*, 2002, **74**, 6139–6144.
6 A. K. Yetisen, M. S. Akram and C. R. Lowe, *Lab Chip*, 2013, **13**, 2210–2251.
7 E. Fu and C. Downs, *Lab Chip*, 2017, **17**, 614–628.
8 X. Li, D. R. Ballerini and W. Shen, *Biomicrofluidics*, 2012, **6**, 011301.
9 Y. Yang, E. Noviana, M. P. Nguyen, B. J. Geiss, D. S. Dandy and C. S. Henry, *Anal. Chem.*, 2017, **89**, 71–91.
10 K. Yamada, H. Shibata, K. Suzuki and D. Citterio, *Lab Chip*, 2017, **17**, 1206–1249.
11 A. Nilghaz, D. Ballerini and W. Shen, *Biomicrofluidics*, 2013, **7**, 051501.
12 G. M. Walker and D. J. Beebe, *Lab Chip*, 2002, **2**, 131–134.
13 E. Berthier and D. J. Beebe, *Lab Chip*, 2007, **7**, 1475–1478.
14 M. W. Toepke, V. V. Abhyankar and D. J. Beebe, *Lab Chip*, 2007, **7**, 1449–1453.
15 S.-J. Kim, S. Paczesny, S. Takayama and K. Kurabayashi, *Anal. Chem.*, 2013, **85**, 6902–6907.
16 B. Zhao, J. S. Moore and D. J. Beebe, *Science*, 2001, **291**, 1023–1026.
17 B. P. Casavant, E. Berthier, A. B. Theberge, J. Berthier, S. I. Montanez-Sauri, L. L. Bischel, K. Brakke, C. J. Hedman, W. Bushman, N. P. Keller and D. J. Beebe, *Proc. Natl. Acad. Sci. U. S. A.*, 2013, **110**, 10111–10116.
18 J. C. T. Eijkel and A. van den Berg, *Lab Chip*, 2005, **5**, 1202–1209.
19 B. S. Gallardo, V. K. Gupta, F. D. Eagerton, L. I. Jong, V. S. Craig, R. R. Shah and N. L. Abbott, *Science*, 1999, **283**, 57–60.
20 M. W. J. Prins, W. J. J. Welters and J. W. Weekamp, *Science*, 2001, **291**, 277–280.
21 F. He and S. R. Nugen, *Microfluid. Nanofluid.*, 2014, 1–8.
22 H. Cho, H.-Y. Kim, J. Y. Kang and T. S. Kim, *J. Colloid Interface Sci.*, 2007, **306**, 379–385.
23 A. Kazemzadeh, P. Ganesan, F. Ibrahim, S. He and M. J. Madou, *PLoS One*, 2013, **8**, e73002.
24 M. R. McNeely, M. K. Sputea, N. A. Tusneem and A. R. Oliphant, *J. Assoc. Lab. Autom.*, 1999, **4**, 1–4.
25 J. Choi, D. Kang, S. Han, S. B. Kim and J. A. Rogers, *Adv. Healthcare Mater.*, 2017, **6**, 1601355.
26 R. Safavieh and D. Juncker, *Lab Chip*, 2013, **13**, 4180–4189.
27 R. L. Columbus, *US Pat.*, 4233029, 1980.
28 E. Delamarche, D. Juncker and H. Schmid, *Angew. Chem., Int. Ed.*, 2005, **17**, 2911–2933.
29 R. L. Columbus, *US Pat.*, 4271119, 1981.
30 R. L. Columbus, *US Pat.*, 4426451, 1984.
31 R. Shartle, D. Besemer and M. Gorin, *US Pat.*, 5230866, 1993.
32 I. Gibbons, R. S. Hillman and C. R. Robertson, *US Pat.*, 4868129, 1989.
33 P. J. Pouletty and T. Ingalz, *US Pat.*, 5135872, 1992.
34 K. F. Buechler, *US Pat.*, 5458852, 1995.

35 R. L. Columbus, *US Pat.*, 4618476, 1986.
36 A. Manz, N. Graber and H. M. Widmer, *Sens. Actuators, B*, 1990, **1**, 244–248.
37 E. Kim, Y. Xia and G. M. Whitesides, *Nature*, 1995, **376**, 581–584.
38 E. Delamarche, A. Bernard, H. Schmid, B. Michel and H. Biebuyck, *Science*, 1997, **276**, 779–781.
39 P. Man, C. Mastrangelo, M. Burns and D. Burke, *Proceedings of The Eleventh Annual International Workshop on Micro Electro Mechanical Systems, MEMS*, 1998, vol. 1998, pp. 45–50.
40 N. Goedecke, J. Eijkel and A. Manz, *Lab Chip*, 2002, **2**, 219–223.
41 W. Wu and A. Manz, *RSC Adv.*, 2015, **5**, 70737–70742.
42 M. I. Mohammed and M. P. Y. Desmulliez, *Microsyst. Technol.*, 2013, 1–10.
43 M.-I. Mohammed and M. P. Y. Desmulliez, *J. Microelectromech. Syst.*, 2014, **23**, 1408–1416.
44 A. O. Olanrewaju, A. Robillard, M. Dagher and D. Juncker, *Lab Chip*, 2016, **16**, 3804–3814.
45 A. O. Olanrewaju, A. Ng, P. Decorwin-Martin, A. Robillard and D. Juncker, *Anal. Chem.*, 2017, **89**, 6846–6853.
46 J. Jurin, *Philosophical Transactions*, 1717, **30**, 739–747.
47 T. Young, *et al.*, *Philos. Trans. R. Soc. London*, 1805, **95**, 65–87.
48 E. Delamarche, A. Bernard, H. Schmid, A. Bietsch, B. Michel and H. Biebuyck, *J. Am. Chem. Soc.*, 1998, **120**, 500–508.
49 E. Kim and G. M. Whitesides, *J. Phys. Chem. B*, 1997, **101**, 855–863.
50 M. Dong and I. Chatzis, *J. Colloid Interface Sci.*, 1995, **172**, 278–288.
51 P. Concus and R. Finn, *Proc. Natl. Acad. Sci. U. S. A.*, 1969, **63**, 292–299.
52 H. Bruus, *Lecture Notes in Theoretical Microfluidics*, Department of Micro and Nanotechnology, Technical University of Denmark, 3rd edn, 2006, p. 31.
53 H. Bruus, *Lecture Notes in Theoretical Microfluidics*, Department of Micro and Nanotechnology, Technical University of Denmark, 3rd edn, 2006, p. 100.
54 E. W. Washburn, *Phys. Rev.*, 1921, **17**, 273–283.
55 H. Bruus, *Lecture Notes in Theoretical Microfluidics*, Department of Micro and Nanotechnology, Technical University of Denmark, 3rd edn, 2006, p. 47.
56 J. Melin, N. Roxhed, G. Gimenez, P. Griss, W. van der Wijngaart and G. Stemme, *Sens. Actuators, B*, 2004, **100**, 463–468.
57 M. Zimmermann, P. Hunziker and E. Delamarche, *Microfluid. Nanofluid.*, 2008, **5**, 395–402.
58 L. Gervais and E. Delamarche, *Lab Chip*, 2009, **9**, 3330–3337.
59 Y. Xia and G. M. Whitesides, *Annu. Rev. Mater. Res.*, 1998, **28**, 153–184.
60 D. Qin, Y. Xia and G. M. Whitesides, *Nat. Protoc.*, 2010, **5**, 491.
61 S. H. Kim, Y. Yang, M. Kim, S. W. Nam, K. M. Lee, N. Y. Lee, Y. S. Kim and S. Park, *Adv. Funct. Mater.*, 2007, **17**, 3493–3498.
62 J. Wang, H. Ahmad, C. Ma, Q. Shi, O. Vermesh, U. Vermesh and J. Heath, *Lab Chip*, 2010, **10**, 3157–3162.
63 C. F. Carlborg, T. Haraldsson, K. Öberg, M. Malkoch and W. van der Wijngaart, *Lab Chip*, 2011, **11**, 3136–3147.
64 J. Hansson, H. Yasuga, T. Haraldsson and W. van der Wijngaart, *Lab Chip*, 2016, **16**, 298–304.
65 H. Bruus, *Lecture Notes in Theoretical Microfluidics*, Department of Micro and Nanotechnology, Technical University of Denmark, 3rd edn, 2006, p. 94.
66 Critical Surface Tension and Contact Angle with Water for Various Polymers, https://www.accudynetest.com/polytable_03html.Lastvisitedon2018/05/05.
67 D. Bodas and C. Khan-Malek, *Sens. Actuators, B*, 2007, **123**, 368–373.
68 D. Wild, *The immunoassay handbook: theory and applications of ligand binding, ELISA and related techniques*, Elsevier, 4th edn, 2013, pp. 7–10.
69 D. Wild, *The immunoassay handbook: theory and applications of ligand binding, ELISA and related techniques*, Elsevier, 4th edn, 2013, pp. 29–223.
70 S. Huang, K. Abe, S. Bennett, T. Liang, P. D. Ladd, L. Yokobe, C. E. Anderson, K. Shah, J. Bishop, M. Purfield, P. C. Kauffman, S. Paul, A. E. Welch, B. Strelitz, K. Follmer, K. Pullar, L. Sanchez-Erebia, E. Gerth-Guyette, G. Domingo, E. Klein, J. A. Englund, E. Fu and P. Yager, *Anal. Chem.*, 2017, **89**, 5776–5783.
71 G. A. Lenk, G. Stemme and N. Roxhed, *Proceedings of The 18th International Conference on Miniaturized Systems for Chemistry and Life Sciences (μTAS)*, San Antonio, USA, 2014, pp. 216–218.
72 T. J. Clark, P. H. McPherson and K. F. Buechler, *Point Care*, 2002, **1**, 42–46.
73 M. Wolf, D. Juncker, B. Michel, P. Hunziker and E. Delamarche, *Biosens. Bioelectron.*, 2004, **19**, 1193–1202.
74 P. Novo, V. Chu and J. P. Conde, *Biosens. Bioelectron.*, 2014, **57**, 284–291.
75 P. B. Lillehoj, F. Wei and C.-M. Ho, *Lab Chip*, 2010, **10**, 2265–2270.
76 J. Kai, A. Puntambekar, N. Santiago, S. H. Lee, D. W. Sehy, V. Moore, J. Han and C. H. Ahn, *Lab Chip*, 2012, **12**, 4257–4262.
77 J. Stucki, M. Hitzbleck and E. Delamarche, *Proceedings of The 16th International Conference on Miniaturized Systems for Chemistry and Life Sciences (μTAS)*, Okinawa, Japan, 2012, pp. 1927–1929.
78 Y. Temiz, M. Lim and E. Delamarche, *Progress in Biomedical Optics and Imaging - Proceedings of SPIE*, 2016, p. 97050Z.
79 R. Epifania, R. R. G. Soares, I. F. Pinto, V. Chu and J. P. Conde, *Sens. Actuators, B*, 2018, **265**, 452–458.
80 J. Berthier, D. Gosselin, A. Pham, G. Delapierre, N. Belgacem and D. Chaussy, *Langmuir*, 2016, **32**, 915–921.
81 L. Gervais, M. Hitzbleck and E. Delamarche, *Biosens. Bioelectron.*, 2011, **27**, 64–70.
82 M. Hitzbleck, L. Gervais and E. Delamarche, *Lab Chip*, 2011, **11**, 2680–2685.

83 M. Pla-Roca and D. Juncker, in *Methods Mol. Biol.*, ed. A. Khademhosseini, K.-Y. Suh and M. Zourob, Humana Press, Totowa, NJ, 2010, pp. 177–194.
84 M. Zimmermann, H. Schmid, P. Hunziker and E. Delamarche, *Lab Chip*, 2007, **7**, 119–125.
85 R. Safavieh, A. Tamayol and D. Juncker, *Microfluid. Nanofluid.*, 2014, **18**, 357–366.
86 M. Zimmermann, S. Bentley, H. Schmid, P. Hunziker and E. Delamarche, *Lab Chip*, 2005, **5**, 1355–1359.
87 N. S. Lynn and D. S. Dandy, *Lab Chip*, 2009, **9**, 3422.
88 X. Wang, J. A. Hagen and I. Papautsky, *Biomicrofluidics*, 2013, **7**, 014107.
89 B. M. Cummins, R. Chinthapatla, B. Lenin, F. S. Ligler and G. M. Walker, *Technology*, 2017, **05**, 21–30.
90 Y. M. Bae, K.-H. Lee, J. Yang, D. Heo and H. J. Cho, *Jpn. J. Appl. Phys.*, 2014, **53**, 067201.
91 Y.-C. Lee and W.-H. Hsieh, *Sens. Actuators, B*, 2014, **202**, 1078–1087.
92 Y. Oyama, T. Osaki, K. Kamiya, M. Sawai, M. Sakai and S. Takeuchi, *Sens. Actuators, B*, 2017, **240**, 881–886.
93 D. Juncker, H. Schmid, A. Bernard, I. Caelen, B. Michel, N. de Rooij and E. Delamarche, *J. Micromech. Microeng.*, 2001, **11**, 532–541.
94 D. Juncker, H. Schmid and E. Delamarche, *Proceedings of the 9th International Conference on Miniaturized Systems for Chemistry and Life Sciences (μTAS)*, Boston, USA, 2005, pp. 596–598.
95 P. Vulto, S. Podszun, P. Meyer, C. Hermann, A. Manz and G. A. Urban, *Lab Chip*, 2011, **11**, 1596–1602.
96 E. Yildirim, S. J. Trietsch, J. Joore, A. van den Berg, T. Hankemeier and P. Vulto, *Lab Chip*, 2014, **14**, 3334–3340.
97 O. Gökçe, S. Castonguay, Y. Temiz, T. Gervais and E. Delamarche, *Proceedings of The 20th International Conference on Miniaturized Systems for Chemistry and Life Sciences (μTAS)*, Dublin, Ireland, 2016, pp. 9–10.
98 J. M. Chen, P.-C. Huang and M.-G. Lin, *Microfluid. Nanofluid.*, 2007, **4**, 427–437.
99 A. Glière and C. Delattre, *Sens. Actuators, A*, 2006, **130**, 601–608.
100 M. Hitzbleck, L. Avrain, V. Smekens, R. D. Lovchik, P. Mertens and E. Delamarche, *Lab Chip*, 2012, **12**, 1972–1978.
101 K. Kistrup, C. E. Poulsen, P. F. Østergaard, K. B. Haugshøj, R. Taboryski, A. Wolff and M. F. Hansen, *J. Micromech. Microeng.*, 2014, **24**, 125007.
102 V. A. Papadimitriou, L. I. Segerink, A. Van den Berg and J. C. T. Eijkel, *Anal. Chim. Acta*, 2018, **1000**, 232–238.
103 M. Hitzbleck and E. Delamarche, *Micromachines*, 2013, **4**, 1–8.
104 S. Cesaro-Tadic, G. Dernick, D. Juncker, G. Buurman, H. Kropshofer, B. Michel, C. Fattinger and E. Delamarche, *Lab Chip*, 2004, **4**, 563–569.
105 B. Lutz, T. Liang, E. Fu, S. Ramachandran, P. Kauffman and P. Yager, *Lab Chip*, 2013, **13**, 2840–2847.
106 K. F. Buechler, P. McPherson, J. Anderberg, K. Nakamura, S. Lesefko and B. Noar, *Proceedings of the 5th International Conference on Miniaturized Systems for Chemistry and Life Sciences (μTAS)*, Monterrey, USA, 2001, pp. 42–44.
107 B. Michel André Bernard and E. Delamarche, *Anal. Chem.*, 2000, **73**, 8–12.
108 P. Novo, F. Volpetti, V. Chu and J. P. Conde, *Lab Chip*, 2013, **13**, 641–645.
109 M. Zimmermann, P. Hunziker and E. Delamarche, *Biomed. Microdevices*, 2009, **11**, 1–8.
110 C. Jönsson, M. Aronsson, G. Rundström, C. Pettersson, I. Mendel-Hartvig, J. Bakker, E. Martinsson, B. Liedberg, B. MacCraith, O. Öhman and J. Melin, *Lab Chip*, 2008, **8**, 1191–1197.
111 S.-J. Kim, S. Paczesny, S. Takayama and K. Kurabayashi, *Lab Chip*, 2013, **13**, 2091–2098.
112 E. Fu, T. Liang, J. Houghtaling, S. Ramachandran, S. A. Ramsey, B. Lutz and P. Yager, *Anal. Chem.*, 2011, **83**, 7941–7946.
113 C. D. Chin, T. Laksanasopin, Y. K. Cheung, D. Steinmiller, V. Linder, H. Parsa, J. Wang, H. Moore, R. Rouse, G. Umviligihozo, E. Karita, L. Mwambarangwe, S. L. Braunstein, J. van de Wijgert, R. Sahabo, J. E. Justman, W. El-Sadr and S. K. Sia, *Nat. Med.*, 2011, **17**, 1015–1019.
114 E. Fu, S. A. Ramsey, P. Kauffman, B. Lutz and P. Yager, *Microfluid. Nanofluid.*, 2010, **10**, 29–35.
115 M. I. Mohammed and M. P. Y. Desmulliez, *Biosens. Bioelectron.*, 2014, **61**, 478–484.
116 N. Ramalingam, H.-B. Liu, C.-C. Dai, Y. Jiang, H. Wang, Q. Wang, K. M. Hui and H.-Q. Gong, *Biomed. Microdevices*, 2009, **11**, 1007.
117 H. Tachibana, M. Saito, K. Tsuji, K. Yamanaka, L. Q. Hoa and E. Tamiya, *Sens. Actuators, B*, 2015, **206**, 303–310.
118 H. Tachibana, M. Saito, S. Shibuya, K. Tsuji, N. Miyagawa, K. Yamanaka and E. Tamiya, *Biosens. Bioelectron.*, 2015, **74**, 725–730.
119 A. Sposito, V. Hoang and D. L. DeVoe, *Lab Chip*, 2016, **16**, 3524–3531.
120 N. Ramalingam, M. E. Warkiani, N. Ramalingam, G. Keshavarzi, L. Hao-Bing and T. G. Hai-Qing, *Biomed. Microdevices*, 2016, **18**, 68.
121 D. A. Bartholomeusz, R. W. Boutté and J. D. Andrade, *J. Microelectromech. Syst.*, 2005, **14**, 1364–1374.
122 J. I. Martínez-López, M. Mojica, C. A. Rodríguez and H. R. Siller, *Sensors*, 2016, **16**, 705.
123 M. I. Mohammed, E. Abraham and M. P. Y. Desmulliez, *J. Micromech. Microeng.*, 2013, **23**, 035034.
124 S. Yan, Y. Zhu, S.-Y. Tang, Y. Li, Q. Zhao, D. Yuan, G. Yun, J. Zhang, S. Zhang and W. Li, *Electrophoresis*, 2018, **39**, 957–964.
125 D. Lim, Y. Kamotani, B. Cho, J. Mazumder and S. Takayama, *Lab Chip*, 2003, **3**, 318–323.
126 K. Sugioka, J. Xu, D. Wu, Y. Hanada, Z. Wang, Y. Cheng and K. Midorikawa, *Lab Chip*, 2014, **14**, 3447–3458.
127 A. K. Au, W. Huynh, L. F. Horowitz and A. Folch, *Angew. Chem., Int. Ed.*, 2016, **55**, 3862–3881.
128 S. Waheed, J. M. Cabot, N. P. Macdonald, T. Lewis, R. M. Guijt, B. Paull and M. C. Breadmore, *Lab Chip*, 2016, **16**, 1993–2013.

129 B. Gross, S. Y. Lockwood and D. M. Spence, *Anal. Chem.*, 2017, **89**, 57–70.
130 N. P. Macdonald, J. M. Cabot, P. Smejkal, R. M. Guijt, B. Paull and M. C. Breadmore, *Anal. Chem.*, 2017, **89**, 3858–3866.
131 H. Gong, A. T. Woolley and G. P. Nordin, *Lab Chip*, 2016, **16**, 2450–2458.
132 H. Gong, B. P. Bickham, A. T. Woolley and G. P. Nordin, *Lab Chip*, 2017, **17**, 2899–2909.
133 S. Smith, D. Mager, A. Perebikovsky, E. Shamloo, D. Kinahan, R. Mishra, S. T. Delgado, H. Kido, S. Saha, J. Ducrée, M. Madou, K. Land and J. Korvink, *Micromachines*, 2016, **7**, 22.
134 B. Suman and R. Savino, *J. Thermophys. Heat Transfer*, 2011, **25**, 553–560.
135 C. J. Morris and B. A. Parviz, *J. Micromech. Microeng.*, 2008, **18**, 015022.
136 F. Shao, T. W. Ng, J. Fu, W. Shen and W. Y. L. Ling, *J. Colloid Interface Sci.*, 2011, **363**, 425–430.
137 Y. Ding, L. Hong, B. Nie, K. S. Lam and T. Pan, *Lab Chip*, 2011, **11**, 1464–1469.
138 J. Lippai, R. Sanka, A. Lashkaripour and D. Densmore, *The Proceedings of the 9th International Workshop on Bio-Design Automation*, 2017.
139 A. O. Olanrewaju, M. Yafia, M. Beaugrand, F. Possel and D. Juncker, *Proceedings of the 21st International Conference on Miniaturized Systems for Chemistry and Life Sciences (μTAS)*, Savannah, USA, 2017, pp. 73–74.